

**A Wavelet Packet Based Sifting Process and  
Its Application for Structural Health Monitoring**

by

**Abhijeet Dipak Shinde**

**A Thesis**

**Submitted to the Faculty of**

**WORCESTER POLYTECHNIC INSTITUTE**

**in partial fulfillment of the requirements for the**

**Degree of Master of Science**

in

**Mechanical Engineering**

by

---

**Abhijeet Dipak Shinde**

**August 2004**

**Approved:**

---

Prof. Zhikun Hou  
Thesis Advisor

---

Prof. Mikhail Dimentberg  
Committee Member

---

Prof. Michael Demetriou  
Committee Member

---

Prof. John Sullivan  
Graduate Committee Representative

---

Prof. John Hall  
Committee Member

## ABSTRACT

In this work an innovative wavelet packet based sifting process for signal decomposition has been developed and its application for health monitoring of time-varying structures is presented. With the proposed sifting process, a signal can be decomposed into its mono-frequency components by examining the energy content in the wavelet packet components of a signal, and imposing certain decomposition criteria. The method is illustrated for simulation data of a linear three degree-of-freedom spring-mass-damper system and the results are compared with those obtained using the empirical mode decomposition (EMD) method. Both methods provide good approximations, as compared with the exact solution for modal responses from a conventional modal analysis. Incorporated with the classical Hilbert transform, the proposed sifting process may be effectively used for structural health monitoring by monitoring instantaneous modal parameters of the structure for both, cases of abrupt structural stiffness loss and progressive stiffness degradation. The effectiveness of this method for practical application is evaluated by applying the methodology for experimental data and the results obtained matched with the field observations. The proposed methodology has shown better results in a comparison study which is done to evaluate performance of the proposed approach with other available SHM techniques, namely EMD technique and Continuous Wavelet Transform (CWT) method, for cases characterized by different damage scenarios and noise conditions.

## ACKNOWLEDGEMENTS

It gives me an immense pleasure to present the thesis report in its completed form. First of all, I would like to thank Prof. Hou, for his extensive support as a thesis advisor. Without his timely advice and thorough knowledge in structural dynamics and earthquake engineering, the research would not have been accomplished such a great success. I am extremely thankful for his support.

I thank Prof. Suzuki and his team at Kyoto University, Japan for providing the experimental data of a test conducted on a two-story wooden structure. I would like to thank Prof. Demetriou, Prof. Dimentberg, Prof. Hall, and Prof. Sullivan for being in my thesis committee and their valuable suggestions about thesis report. I would like to express my gratitude towards Adriana, my research group partner, for her help, whom I bothered since the first day of starting my research and at each time she helped me without any hesitation. Discussion with her and Wei at weekly meetings helped a lot to get better understanding of the concepts.

I thank Sagar and Siju for their affection and the memorable moments we shared with each other. I would like to thank Jayant, Anjali, Sachin, Viren, Rohit, Souvik, Gana, Mandeep, Ryan, Elham, Taraneh, and Dave who always supported me, directly or indirectly during the last two years. I thank my friends in India for being there for me whenever I needed. I thank ladies in the ME office, the best staff in WPI, Barbara Edilberti, Barbara Fuhman, Janice and Pam for all of their kindness and cooperation.

Last, but the most important, I am extremely grateful to my parents and my brother and sister, Ritesh and Reshma, who are my inspiration and strength and even being miles away from me, encouraged to accomplish each and every task.

*To Aai - Pappa*

# TABLE OF CONTENTS

|   |      |
|---|------|
| List of Figures   | iv   |
| List of Tables  | viii |
| Nomenclature  | ix   |
| 1. Introduction   | 1    |
| 1.1 Structural Health Monitoring Overview               | 1    |
| 1.1.1 Types of Damage                                   | 1    |
| 1.1.2 Types of Damage Detection Techniques              | 2    |
| 1.1.3 Levels of Structural Health Monitoring            | 3    |
| 1.2 Damage Identification Techniques                    | 4    |
| 1.2.1 Change in Modal Parameters                        | 4    |
| 1.2.1.1 Change in Natural Frequency                     | 4    |
| 1.2.1.2 Change in Mode Shapes                           | 5    |
| 1.2.2 Methods based on Dynamic Flexibility Measurements | 6    |
| 1.2.3 Model Update Methods                              | 6    |
| 1.2.4 Neural Network based Methods                      | 7    |
| 1.2.5 Pattern Recognition Techniques                    | 8    |
| 1.2.6 Kalman Filter Technique                           | 9    |
| 1.2.7 Statistical Approach                              | 10   |
| 1.3 Signal Processing Methods                           | 11   |
| 1.3.1 Fourier Analysis                                  | 11   |
| 1.3.2 Wavelet Analysis                                  | 13   |
| 1.3.2.1 Continuous Wavelet Transform                    | 13   |
| 1.3.2.2 Discrete Wavelet Transform                      | 14   |
| 1.3.2.3 Wavelet Packet Transform                        | 16   |
| 1.3.3 Hilbert-Huang Analysis                            | 17   |
| 1.4 Motivation  | 20   |
| 2 A Wavelet Packet based Sifting Process                | 22   |

|         |   |    |
|---------|---|----|
| 2.1     | Mathematical Background   | 22 |
| 2.1.1   | Wavelet Packet Transform  | 22 |
| 2.1.2   | Wavelet Packet Node Energy and Entropy Index                    | 23 |
| 2.2     | Methodology   | 24 |
| 2.3     | Validation of the Wavelet Packet based Sifting Process          | 25 |
| 2.3.1   | Simulation Model  | 26 |
| 2.3.2   | Model Parameters  | 27 |
| 2.3.3   | Validation  | 28 |
| 2.4     | Comparison of the EMD method and Wavelet Packet Sifting Process | 32 |
| 3       | Application for Structural Health Monitoring                    | 37 |
| 3.1     | Numerical Studies   | 39 |
| 3.1.1   | Case Study 1: Detection of Sudden Damage                        | 40 |
| 3.1.1.1 | Effect of Measurement Noise                                     | 42 |
| 3.1.1.2 | Forced Vibration Response                                       | 43 |
| 3.1.1.3 | Effect of Damage Severity                                       | 44 |
| 3.1.2   | Case Study 2: Detection of Progressive Damage                   | 46 |
| 3.2     | Experimental Validation   | 48 |
| 3.2.1   | Shaking Table Test  | 48 |
| 3.2.2   | Methodology   | 49 |
| 3.2.3   | Results for Experimental Data and Discussion                    | 52 |
| 4       | Comparison Study  | 58 |
| 4.1     | Methodology   | 58 |
| 4.1.1   | Continuous Wavelet Transform Technique                          | 58 |
| 4.1.2   | Wavelet Packet based Sifting Process Technique                  | 59 |
| 4.1.3   | Empirical Mode Decomposition Technique                          | 59 |
| 4.2     | Results   | 60 |
| 4.2.1   | Simulation Setup  | 60 |
| 4.2.2   | Implementation of the Methods                                   | 62 |
| 4.2.3   | Simulation Results  | 62 |
| 4.2.3.1 | Progressive Damage  | 63 |

|   |    |
|---|----|
| 4.2.3.2 Sudden Damage                                   | 66 |
| 4.2.4 Damage Detection in Presence of Measurement Noise | 67 |
| 4.3 Discussion  | 70 |
| 4.3.1 Interpretation of the Methods                     | 70 |
| 4.3.2 Robustness to Noise                               | 71 |
| 4.3.3 Sensitivity to the Damage Type                    | 71 |
| 5 Conclusion  | 74 |
| 6 Future Work   | 76 |
| References  | 77 |
| Appendix-A The Modified EMD Method                      | 83 |

## List of Figures:

| <b>Figure</b> |   | <b>Page</b> |
|---------------|---|-------------|
| 1.1           | Discrete wavelet transform decomposition tree   | 15          |
| 1.2           | Wavelet packet decomposition tree   | 16          |
| 2.1           | 3DOF mass-spring-damper system used in the simulation study   | 26          |
| 2.2           | Decomposition of an acceleration response signal of a linear 3DOF system by the proposed wavelet-packet sifting process.              | 29          |
| 2.3           | Fourier spectra of the original signal and its decomposed components  | 30          |
| 2.4           | Errors between the reconstructed signal and the original signal   | 31          |
| 2.5           | Comparison of modal responses obtained from wavelet packet sifting process with the results obtained by EMD method and modal analysis | 32          |
| 2.6           | Decomposition of a chirp signal by the EMD method   | 33          |
| 2.7           | Decomposition of a chirp signal by the propose sifting process  | 34          |
| 2.8           | Decomposition of an impulse acceleration response signal of a SDOF linear damped system by the EMD method                             | 35          |
| 2.9           | Decomposition of an impulse acceleration response signal of a linear SDOF system by the proposed wavelet packet sifting process       | 35          |
| 3.1           | Results from a case study for sudden damage using a free vibration signal   | 41          |
| 3.2           | Instantaneous normalized 3 <sup>rd</sup> mode shape at M2 and M3  | 41          |

|             |   |    |
|-------------|---|----|
|             | indicating sudden damage at $t = 15\text{sec}$  |    |
| <b>3.3</b>  | Sudden damage detection in presence of measurement noise  | 42 |
| <b>3.4</b>  | Instantaneous normalized 3 <sup>rd</sup> mode shapes at M2 and M3 in presence of measurement noise  | 43 |
| <b>3.5</b>  | Sudden damage detection using a forced vibration signal with random noise of 0.03 standard deviation.   | 44 |
| <b>3.6</b>  | Comparison of instantaneous frequency of 3 <sup>rd</sup> mode for detection of damage of 5%, 10%, and 15% sudden stiffness loss of K2.                  | 45 |
| <b>3.7</b>  | Comparison of normalized instantaneous modal shapes of the 3 <sup>rd</sup> mode for detection of damage of 5%, 10%, and 15% sudden stiffness loss of K2 | 45 |
| <b>3.8</b>  | Results from a case study for monitoring progressive damage   | 47 |
| <b>3.9</b>  | Normalized 3 <sup>rd</sup> mode shape results for monitoring progressive damage   | 48 |
| <b>3.10</b> | Two-story wooden structure(left) and observed damage (right)  | 49 |
| <b>3.11</b> | CWT map of the El Centro earthquake signal  | 51 |
| <b>3.12</b> | CWT map of the acceleration response measured at M1.  | 51 |
| <b>3.13</b> | Excitation signal, first-floor acceleration signal and its natural frequency component at load level of $1\text{m/s}^2$                                 | 54 |
| <b>3.14</b> | Phase angle variation at different load levels  | 54 |
| <b>3.15</b> | Instantaneous frequency variations at different load levels   | 55 |
| <b>3.16</b> | Instantaneous frequency variations at consecutive load levels   | 56 |

|             |   |    |
|-------------|---|----|
| <b>4.1</b>  | Stiffness history for: a) damage scenario 1, b) damage scenario 2   | 61 |
| <b>4.2</b>  | The normalized instantaneous mode shape for the first vibration mode, damage scenario 1, no measurement noise.          | 64 |
| <b>4.3</b>  | The instantaneous damped natural frequency for the first vibration mode, damage scenario 1, no measurement noise.       | 64 |
| <b>4.4</b>  | The normalized instantaneous mode shape for the first vibration mode, damage scenario 2, no measurement noise.          | 65 |
| <b>4.5</b>  | The instantaneous damped natural frequency for the second vibration mode, damage scenario 1, no measurement noise.      | 65 |
| <b>4.6</b>  | The normalized instantaneous mode shape for the first vibration mode, damage scenario 2, no measurement noise.          | 66 |
| <b>4.7</b>  | The instantaneous damped natural frequency for the first vibration mode, damage scenario 1, no measurement noise.       | 67 |
| <b>4.8</b>  | The normalized instantaneous mode shape for the first vibration mode, damage scenario 1, measurement noise level=5%.    | 68 |
| <b>4.9</b>  | The instantaneous damped natural frequency for the first vibration mode, damage scenario 1, measurement noise level=5%. | 68 |
| <b>4.10</b> | The normalized instantaneous mode shape for the first vibration mode, damage scenario 2, measurement noise level=5%.    | 69 |
| <b>4.11</b> | The instantaneous damped natural frequency for the first vibration mode, damage scenario 2, measurement noise level=5%. | 69 |

|           |   |    |
|-----------|---|----|
| <b>A1</b> | Decomposition results obtained by EMD method          | 84 |
| <b>A2</b> | Decomposition results obtained by modified EMD method | 84 |

## List of Tables:

| <b>Table</b> |   | <b>Page</b> |
|--------------|---|-------------|
| <b>2.1</b>   | Percentage energy contribution                        | 29          |
| <b>3.1</b>   | Percentage energy contribution at various load levels | 52          |

## **Nomenclature:**

$a$  = Dilation parameter

$a(t)$  = Instantaneous amplitude

$A_i(t)$  = Approximation component of the discrete wavelet decomposition tree at  $i^{\text{th}}$  level

$b$  = Translation parameter

$c_i(t)$  =  $i^{\text{th}}$  Intrinsic Mode Function (IMF)

$C_i$  =  $i^{\text{th}}$  Damping element

$D_i(t)$  = Detail component of the discrete wavelet decomposition tree at  $i^{\text{th}}$  level

$e_n$  = Nodal entropy in wavelet packet tree

$E.I.$  = Entropy Index

$F(t)$  = External force matrix

$H(\omega)$  = Fourier transform of a signal

$K_i$  =  $i^{\text{th}}$  Stiffness element

$M_i$  =  $i^{\text{th}}$  Mass element

$r_n$  = Residue

$t$  = time

$W_f(a, b)$  = Wavelet transform of a signal

$X_{norm}^{(i)}$  =  $i^{\text{th}}$  normalized mode shape vector

$X(t)$  = Mass displacement matrix

$\dot{X}(t)$  = Mass velocity matrix

$\ddot{X}(t)$  = Mass acceleration matrix

$z(t)$  = Analytic function

$\vartheta(t)$  = Instantaneous phase angle

$\bar{\Psi}$  = Conjugate of the mother wavelet function  $\Psi$

$\omega(t)$  = Instantaneous frequency

$\omega$  = Natural frequency (rad/sec)

# 1. INTRODUCTION

## 1.1 STRUCTURAL HEALTH MONITORING (SHM) OVERVIEW:

Structural health monitoring has become an evolving area of research in last few decades with increasing need of online monitoring the health of large structures. The damage detection by visual inspection of the structure can prove impractical, expensive and ineffective in case of large structures like multistoried buildings and bridges. This necessitates the development of structural health monitoring system that can effectively detect the occurrence of damage in the structure and can provide information regarding the location as well as severity of damage and possibly the remaining life of the structure. The SHM system analyzes the structural response by excitation due to controlled or uncontrolled loading. The controlled loading may be attributed to impulse excitation whereas the uncontrolled loading may be attributed to the excitation by automobiles on bridge, and a random excitation due to wind loads or an earthquake excitation.

### 1.1.1 Types of Damage:

Damage phenomena in a structure can be classified as linear damage and non-linear damage. Linear damage is a case when the initially linear-elastic structure remains linear-elastic after damage (Doebeling et al, 1996). This is a case when the structure is subjected to a sudden damage of lower intensity. The modal parameters change in this case but the structure still exhibits linear motion after damage. This facilitates to form a simple model of the structure and to derive equations of motion based on an assumption of linear structural properties.

Non-linear damage is a case when the initially linear-elastic structure exhibits non-linear behavior after damage. A fatigue crack initiated in shaft subjected to cyclic loading can be called as a non-linear damage case. The crack opens and closes during every cycle exhibiting non-linear stiffness of the shaft. Most of the damage detection techniques assume linear damage while forming a model of the structure.

### **1.1.2 Types of Damage Detection Techniques:**

Current damage detection methods can be mainly categorized into local damage detection methods and global damage detection methods. In case of local damage detection methods, the approximate location of damage in structure is known and it analyzes the structure locally to detect the damage on or near the surface. The region of the damaged structure needs to be easily accessible to effectively detect the exact location and severity of damage. Some of the examples of the local damage detection techniques are eddy current technique, acoustic or ultrasonic damage detection technique and radio graph technique.

Contrary to the local damage detection methods, global methods do not require prior knowledge of the location of damage in the structure to be analyzed. Global methods monitor the changes in the vibration characteristics of the structure to detect the location and severity of damage. The changes in dynamic properties of the structure may be attributed to the damage occurrence in the structure as the modal parameters comprising natural frequencies, mode shapes and damping ratio are the functions of the physical properties(mass, damping and stiffness) of the structure. Any change in the physical properties results change in the modal parameters.

### **1.1.3 Levels of Structural Health Monitoring:**

Various global damage identification techniques have been developed till date. The effectiveness of each method can be evaluated by the extent of the information obtained about damage. Rytter (1993) proposed a system of classification for damage-identification techniques which defined four levels of damage identification as follows:

Level 1: Determination that damage is present in the structure

Level 2: Determination of the geometric location of the damage

Level 3: Quantification of the severity of the damage

Level 4: Prediction of the remaining service life of the structure

Damage identification techniques used in industrial machinery may be limited to Level 1 technique and is commonly known as fault identification technique, but most of the damage detection techniques implemented in the SHM systems of civil infrastructures are Level 3 or Level 4 techniques.

## **1.2 DAMAGE IDENTIFICATION TECHNIQUES:**

Different types of damage identification methods based on the measurement of the dynamic properties of the structure have been developed till date. These methods can be categorized depending upon the type of data collected from the structure, the parameters monitored to identify damage or technique implemented to identify damage. Some of the methods to quote are methods monitoring changes in modal parameters, matrix update methods, neural network based methods, pattern recognition methods, Kalman filter based methods and methods based on statistical approach. This section summarizes all of the above stated methods.

### **1.2.1 Change in Modal Parameters:**

Any change in dynamic properties of structure cause change in modal properties of the structure including change in natural frequencies, mode shapes and modal damping values. These values can be tracked to get information about damage present in the structure.

#### ***1.2.1.1 Change in Natural Frequency***

Natural frequency of a structure is the function of stiffness and mass of the structural members. Any damage occurred in the structure causes loss of stiffness whereas the mass of the structural members remains the same resulting in the loss of the natural frequency of the structure. Thus a loss in a natural frequency of the structure can be used as an indicator of damage in the structure.

The damage identification with this technique is implemented with two types of approaches. One of the approach models damage mathematically and predicts a natural

frequency of structure. The predicted natural frequency is compared it with the measured natural frequency and damage is identified. This approach was implemented to identify a presence of damage in the structure. Application of this approach for offshore platforms is studied in Osegueda, et al (1992) while Silva & Gomes (1994) demonstrated use of this approach for detecting crack length.

The second approach calculates damage parameters like crack length and location from the frequency shifts thus measure intensity and location of damage in addition to just damage identification as observed in the first approach. Brincker, et al. (1995a) measured resonant frequencies and damping present in a concrete offshore oil platform by applying auto-regressive moving average (ARMA) model to measured acceleration response.

As a natural frequency of a structure is the global property of structure, it cannot give spatial information about damage in the structure and thus only indicate the occurrence of damage and only can be used as a level 1 damage detection technique. Exception to this is a modal response at higher natural frequencies as the mode shapes are associated with local responses at higher modal frequencies.

### ***1.2.1.2 Change in Mode Shapes***

Mode shape information can be utilized to locate damage in the structure and this technique can be implemented as Level 3 damage detection technique. Damage present in structure causes change in a mode shape and relative change in the mode shape can be graphically monitored to locate damage in the structure. The mode-shapes need to be normalized in order to effectively find the location of damage. Apart from graphical

monitoring of relative change in mode shape, Modal Assurance Criteria (MAC) can be utilized to track the location of damage in the structure as described in West (1984).

### **1.2.2 Methods Based on Dynamic Flexibility Measurements**

These methods use the dynamically measured stiffness matrix in order to detect damage. The flexibility matrix of the structure is defined as an inverse of stiffness matrix and each column of the flexibility matrix of the structure corresponds to the displacement pattern of the structure when subjected to unit force at a particular node. The flexibility matrix can be derived by calculating mass-normalized mode shapes and natural frequencies. In case of structure having large number of degrees of freedom (DOF), due to limitations in calculation of all mode shapes and natural frequencies, only significant low- frequency modes and their corresponding natural frequencies are considered.

While implementing this technique, damage is detected by comparing a calculated flexibility matrix obtained by using the modes of the damaged structure to the flexibility matrix obtained with the modes obtained from the undamaged structure. Sometimes, for a comparison of flexibility matrices, a flexibility matrix obtained with Finite Element Model (FEM) of the undamaged structure may be used instead of a measured flexibility matrix of the undamaged structure. This technique can be used as a Level 3 damage detection technique. More information and applications of this technique can be found in Pandey & Biswas (1994, 1995) and Salawu & Williams (1993).

### **1.2.3 Model Update Methods**

This type of techniques uses a structural model and the structural model parameters i.e. mass, stiffness and damping, are calculated from the equations of motion and the

dynamic measurements. The matrices for mass, stiffness and damping in the model are formulated in such a way that the model response will be almost similar to the measured dynamic response of the structure. The matrices are updated with new dynamic measurements and the updated stiffness as well as damping matrix can be compared to the original stiffness and damping matrix respectively to detect the location and intensity of damage in a structure.

Various methods have been developed each with different approach for model updating. Those can be classified in different categories depending on the objective function for minimization problem, constraints placed on the model or numerical method used to accomplish the optimization. For more information about model update methods, reader is referred to Smith & Beattie (1991a) and Zimmerman & Smith (1992).

#### **1.2.4 Neural Network (NN) based Methods**

Neural Network, a concept developed as generalization of mathematical models of human cognition or neural biology, has proven to be an efficient technique for damage detection. According to Haykin(1998), a neural network is a massively parallel distributed processor made of simple processing units, which has a natural propensity for storing experimental knowledge and making it available for use. With its capacity of performing accurate pattern recognition and classification, adaptivity, modeling non-linearity, and learning capabilities, neural networks can be used for SHM in different ways:

1. to model the dynamic behavior of a system or part of the system under control  
(Chen et al, 1995, and Adeli, 2001)

2. to model the restoring forces in civil structures (Liang et al, 1997 and Saadat, 2003)
3. to carry out pattern recognition for fault detection in rotating machinery e.g. gear box failure (Dellomo, 1999), turbo-machinery (Kerezsi & Howard, 1995), and bearing fault detection (Samanta et al, 2004).

Application of neural network model for SHM can also be found in Saadat (2003), where the author used an “Intelligent Parameter Varying” (IPV) technique for health monitoring and damage detection technique that accurately detects the existence, location, and time of damage occurrence without any assumptions about the constitutive nature of structural non-linearity.

The technique in Saadat(2003) was based on the concept of “gray box”, which combined a linear time invariant dynamic model for part of the structure with a neural network model, used to model the restoring forces in a non-linear and time-varying system. The detailed information about the technique can be found in Nelles(2000).

Even if good results obtained with NN techniques, one of the challenges in implementing it for a practical application in SHM is training the network. Recent work in integration of NN with other computational techniques to enhance their performance can be found in Adeli (2001).

### **1.2.5 Pattern Recognition Techniques**

Damage present in the structure causes change in the modal parameters which in turn causes change in the pattern of the structural response. This pattern can be monitored to detect the time, location and intensity of damage. Hera & Hou (2001) successfully detected sudden damage in ASCE benchmark structure by monitoring spikes present in

the higher level details of the acceleration response. A motivation behind this approach was that a sudden damage in structure causes singularity in the acceleration response and this singularity results in a spike in higher level details of the wavelet transform of the signal.

Another pattern recognition method proposed by Los Alamos National Laboratory, NM is based on statistical considerations. It proposed a statistical pattern recognition framework which consists of the assessment of structure's working environment, the acquisition of structural response, the extraction of features sensitive to damage and the development of statistical model which is used for feature discrimination. More information and application of this method can be found in Sohn & Farrar (2001), Sohn et al. (2001a & 2001b), Worden (2002) and Lei et al (2003).

### **1.2.6 Kalman Filter Technique**

Kalman filter technique is the model based technique which implements an optimal recursive data processing algorithm to estimate structural parameters necessary to identify damage in the structure. The parameters with which damage in a structure can be identified (stiffness and damping of the structure) can not be measured directly and in a general practice, acceleration, velocity or displacement of the structure is measured. The Kalman filter technique use a set of equations of motion which relate structural properties with the measured parameters. It works in a predictor-corrector manner i.e. it estimates the value of structural parameter based on the dynamic model and previous measurements and then optimizes the estimated value by comparing it with the value obtained by a measurement model and actual measurements. The optimization of the estimated value is done to minimize the square of the difference between the estimated

and measured value. This technique accounts for the effect of noise introduced during measurement as well as the effect of modeling errors. Kalman filter has been applied for damage detection such as in Lus et al (1999).

### **1.2.7 Statistical Approach**

This new developed technique is fundamentally based on Bayesian approach, a well known theorem in statistical theory. An important advantage of Bayesian approach is that it can handle the non-uniqueness of the model that can appear in the cases with insufficient number of measurements. In order to take care of uncertainties, Beck and Katafygiotis (1998) developed a Bayesian statistical framework for system identification and structural health monitoring. The statistical model was developed to take care of uncertainties introduced due to incomplete test data as a result of limited number of sensors, noise contaminated dynamic test data, modeling errors, insensitiveness of modal parameters to the changes in stiffness, and to describe the class of structural models which include as much prior information as possible to reduce the uncertainties and degree of non-uniqueness.

The method can be used for updating the system probability model to account for above-mentioned uncertainties, and to provide a quantitative assessment of the accuracy of results. The applications of the approach for modal identification can be found in Yuen et al (2002), and Yuen & Katafygiotis (1998), whereas application for ASCE benchmark SHM problem can be found in Yuen et al (2002), and Lam et al (2002).

### 1.3 SIGNAL PROCESSING METHODS

A signal collected from the accelerometers mounted on a structure can not be analyzed directly to draw useful conclusions about damage unless the damage intensity is very high. It needs to be processed in order to extract useful information about the structural parameters and damage. The signal is often transformed to different domains in order to better interpret the physical characteristics inherent in the original signal. The original signal can be reconstructed by performing inverse operation on the transformed signal without any loss of data. The popular methods in signal processing for SHM applications include Fourier Analysis, Wavelet Analysis and Hilbert-Huang Analysis. All of these methods can be distinguished from each other by a way in which it maps the signal and have advantages over one another in terms of applicability for analyzing specific data type. A brief introduction of each method is given below.

#### 1.3.1 Fourier Analysis

Fourier analysis of a signal converts the signal from time domain to frequency domain. Mathematically the Fourier transform of a signal ' $f(t)$ ' can be represented as

$$H(\omega) = \int_{-\infty}^{\infty} f(t)e^{-\omega t} dt \quad (1.1)$$

Where ' $H(\omega)$ ' is the Fourier transform of a signal ' $f(t)$ '. Fourier transform represents the signal in frequency domain and useful information about the frequency content in the signal can be extracted. The plot of the power of Fourier transform versus frequency exhibit peaks at the dominant frequencies present in the signal and the amplitude of the power indicates intensity of the frequency component.

Note here that the Fourier transform of a signal integrates the product of the signal with a harmonic of infinite length and the time information in the signal may be lost or become implicit. If the signal to be analyzed is a non-stationary signal i.e. if the amplitude or frequency is changing abruptly over time, then with the Fourier transform of the signal, this abrupt change in time spread over the whole frequency axis in ' $H(\omega)$ '. Thus the Fourier transform is more appropriate to analyze a stationary signal.

To cope up with a deficiency of losing time information in Fourier transform, a Short-Time-Fourier-Transform (STFT) was developed. STFT uses a sinusoidal window of fixed width to analyze the signal and it shifts along the data to be analyzed in order to retain the time information in the signal. Thus in contrast to only frequency representation ' $H(\omega)$ ' as in case of Fourier transform, STFT employs a time-frequency representation ' $H(\omega, \tau)$ ' of the signal ' $f(t)$ ' as in the following equation 1.2.

$$H(\omega, \tau) = \int f(t)g^*(t-\tau)e^{-i\omega t} dt \quad (1.2)$$

where  $g(t-\tau)$  is a window function. Once the window width is chosen, then the time-frequency resolution obtained remains fixed over entire time-frequency plane and one can either get good time resolution or good frequency resolution in the analysis but not both. More information about the STFT can be found in Allen & Rabiner (1977) and Rioul & Vetterli (1991).

Because of its ability to identify the frequency content and intensity of the frequency component of a signal, significant information about the modal parameters i.e. natural frequency, mode shapes and damping can be extracted from the Fourier transform of the structural response. Various methods of fault diagnosis and damage detection

based on the Fourier transform of the vibration response of the structure can be found in Chiang *et al* (2001).

### **1.3.2 Wavelet Analysis**

Analyzing the response data of general transient nature without knowing when the damage occurred, inaccurate results may be presented by the traditional Fourier analysis due to its time integration over the whole time span. Moreover, damage could develop in progressively such as stiffness degradation due to mechanical fatigue and chemical corrosion and a change in stiffness might never been found. As an extension of the traditional Fourier analysis, wavelet analysis provides a multi-resolution and time-frequency analysis for non-stationary data and therefore can be effectively applied for structural health monitoring.

#### ***1.3.2.1 Continuous Wavelet Transform (CWT)***

The Continuous Wavelet Transform (CWT) of a signal  $f(t)$ ,  $W_f(a,b)$ , is defined as

$$W_f(a,b) = \frac{1}{\sqrt{a}} \int_{-\infty}^{\infty} f(t) * \bar{\Psi}\left(\frac{t-b}{a}\right) dt \quad (1.3)$$

Here ‘ $\bar{\Psi}$ ’ is the conjugate of a mother wavelet function ‘ $\Psi$ ’, ‘ $a$ ’ and ‘ $b$ ’ are called as the dilation parameter and the translation parameter, respectively. Both of the parameters are real and ‘ $a$ ’ must be positive. The mother wavelet ‘ $\Psi$ ’ needs to satisfy certain admissibility condition in order to ensure existence of the inverse wavelet transform.

The dilation parameter ‘ $a$ ’ and the translation parameter ‘ $b$ ’ are also referred as the scaling and shifting parameters respectively and play an important role in the wavelet analysis. By varying the value of translation parameter ‘ $b$ ’, a signal is examined by the

wavelet window piece by piece localized in the neighborhood of ‘ $t=b$ ’ and so the non-stationary nature of the data can be examined which is similar to the Short Time Fourier Transform (STFT). By varying the value of dilation parameter ‘ $a$ ’, the data portion in the neighborhood of ‘ $b$ ’ can be examined in different resolutions and so a time varying frequency content of the signal can be revealed by this multi-resolution analysis, a feature the STFT doesn’t have. The continuous wavelet transform maps the signal on a Time-Scale plane. The concept of scale in Wavelet analysis is similar to the concept of frequency in Time-Frequency analysis. The scale is inversely proportional to the frequency. Performing the inverse wavelet transform on the wavelet transform of a signal, the original signal can be reconstructed without any loss of data. For detailed information of wavelet transform, readers are referred to Rioul & Vetterli (1991) and Daubechies (1992). Early applications of wavelets for damage detection of mechanical systems were summarized in Staszewski (1998).

### ***1.3.2.2 Discrete Wavelet Transform (DWT)***

The computational cost of performing continuous wavelet transform is reduced by implementing Discrete Wavelet Transform (DWT). In DWT the dilation parameter ‘ $a$ ’ and the translation parameter ‘ $b$ ’ are discretized by using the dyadic scale i.e.

$$a = 2^j \quad b = k.2^j \quad j, k \in z \quad (1.4)$$

Here  $z$  is the set of positive integers.

In the case of DWT, the wavelet plays a role of dyadic filter. The DWT analyzes the signal by implementing a wavelet filter of particular frequency band to shift along a time axis. The frequency band of the filter depends on the level of decomposition and by shifting it in the time domain, the local examination of the signal becomes possible. As a

result, the signal can be decomposed into a tree structure with wavelet details and wavelet approximations at various levels as follows

$$f(t) = \sum_{i=1}^{i=j} D_i(t) + A_j(t) \quad (1.5)$$

where  $D_j(t)$  denotes the wavelet detail and  $A_j(t)$  stands for the wavelet approximation at the  $j^{th}$  level, respectively. A graphical representation of DWT of a signal is shown in Figure 1.1.

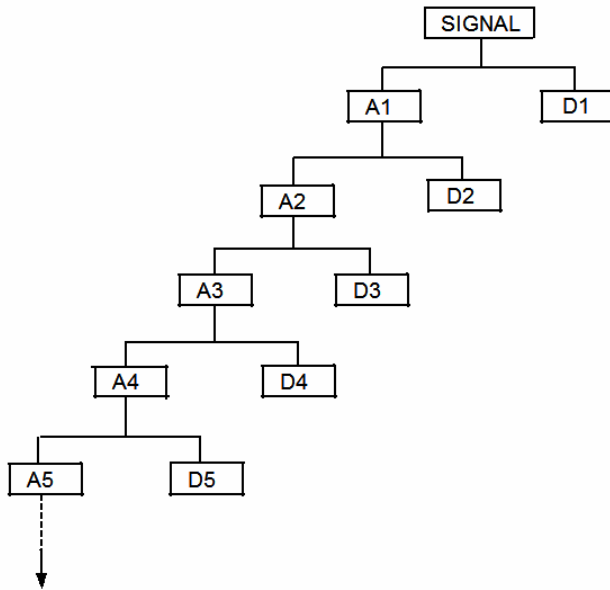


**Figure 1.1 Discrete Wavelet Transform Decomposition Tree**

The DWT decomposition of the signal with each level of decomposition results in halving the time resolution and doubling the frequency resolution. The signal can be easily reconstructed as the dyadic wavelet filter family forms an orthonormal basis (Daubechies, 1999). Recent applications of discrete wavelet transform for structural health monitoring can be found in Hou *et al.* (2000) and Hera and Hou (2003).

### 1.3.2.3 Wavelet Packet Transform

As a result of decomposition of only the approximation component at each level using the dyadic filter bank, the frequency resolution in higher-level e.g. A1 and D1. DWT decompositions in a regular wavelet analysis may be lower. It may cause problems while applying DWT in certain applications, where the important information is located in higher frequency components. The frequency resolution of the decomposition filter may not be fine enough to extract necessary information from the decomposed component of the signal. The necessary frequency resolution can be achieved by implementing a wavelet packet transform to decompose a signal further (Goswami & Chan, 1999). The wavelet packet analysis is similar to the DWT with the only difference that in addition to the decomposition of only the wavelet approximation component at each level, a wavelet detail component is also further decomposed to obtain its own approximation and detail components as shown in Figure 1.2.

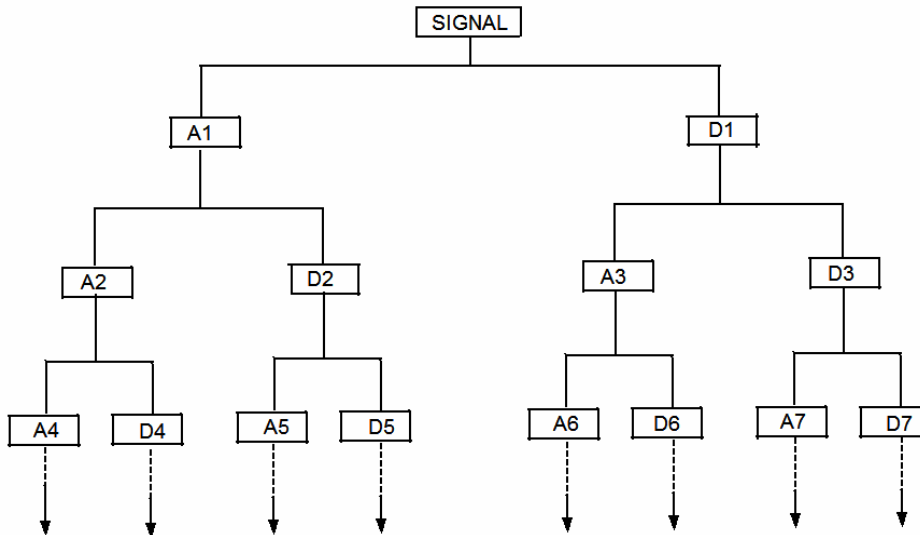


Figure 1.2 Wavelet Packet Decomposition Tree

Each component in this wavelet packet tree can be viewed as a filtered component with a bandwidth of a filter decreasing with increasing level of decomposition and the whole tree can be viewed as a filter bank. At the top of the tree, the time resolution of the WP components is good but at an expense of poor frequency resolution whereas at the bottom of the tree, the frequency resolution is good but at an expense of poor time resolution. Thus with the use of wavelet packet analysis, the frequency resolution of the decomposed component with high frequency content can be increased. As a result, the wavelet packet analysis provides better control of frequency resolution for the decomposition of the signal.

### 1.3.3 Hilbert-Huang Analysis

NASA Goddard Space Flight Center (GSFC) has developed a signal analysis method, called as the Empirical Mode Decomposition (EMD) method, which analyzes the signal by decomposing the signal into its monocomponents, called as Intrinsic Mode Functions (IMF) (Huang et al, 1998). The empirical nature of the approach may be partially attributed to a subjective definition of the envelope and the intrinsic mode function involved in its sifting process. The EMD method used in conjunction with Hilbert Transform is also known as ‘Hilbert-Huang Transform’ (HHT). Because of its effectiveness in analyzing a nonlinear, non-stationary signal, the HHT was recognized as one of the most important discoveries in the field of applied mathematics in NASA history. By the EMD method, discussed in more details later in ‘Section 1.4’, the original signal  $f(t)$  can be represented in terms of IMFs as:

$$f(t) = \sum_{i=1}^n c_i(t) + r_n \quad (1.6)$$

where  $\mathbf{C}_i(t)$  is the  $i^{th}$  Intrinsic Mode Function and  $r_n$  is the residue.

A set of analytic functions can be constructed for these IMFs. The analytic function ‘ $z(t)$ ’ of a typical IMF ‘ $c(t)$ ’ is a complex signal having the original signal ‘ $c(t)$ ’ as the real part and its Hilbert transform of the signal as its imaginary part. By representing the signal in the polar coordinate form one has

$$z(t) = c(t) + jH[c(t)] = a(t).e^{j\phi(t)} \quad (1.7)$$

where ‘ $a(t)$ ’ is the instantaneous amplitude and ‘ $\phi(t)$ ’ is the instantaneous phase function. The instantaneous amplitude ‘ $a(t)$ ’ and is the instantaneous phase function ‘ $\phi(t)$ ’ can be calculated as

$$a(t) = \sqrt{\{c(t)\}^2 + \{H[c(t)]\}^2} \quad (1.8)$$

$$\phi(t) = \tan^{-1} \left\{ \frac{H[c(t)]}{c(t)} \right\} \quad (1.9)$$

The instantaneous frequency of a signal at time  $t$  can be expressed as the rate of change of phase angle function of the analytic function obtained by Hilbert Transform of the signal (Ville, 1948). The expression for instantaneous frequency is given in equation 1.10

$$\omega(t) = \frac{d\phi(t)}{dt} \quad (1.10)$$

Because of a capability of extracting instantaneous amplitude ‘ $a(t)$ ’ and instantaneous frequency ‘ $\omega(t)$ ’ from the signal, this method can be used to analyze a non-stationary vibration signal. In a special case of a single harmonic signal, the phase angle of its Hilbert transform is a linear function of time and therefore its instantaneous frequency is constant and is exactly equal to the frequency of the harmonic. In general, the concept of instantaneous frequency provides an insightful description as how the frequency content of the signal varies with the time. The method can be used for damage detection and

system identification and the relevant applications can be found in Vincent *et al* (1999), Yang & Lei (2000), Yang et al (2003a, 2003b, 2004).

## 1.4 MOTIVATION

The Empirical Mode Decomposition (EMD) method proposed by Huang *et al* (1998) decomposes a signal into IMFs by an innovative sifting process. The IMF is defined as a function which satisfy following two criterion

- (i) The number of extrema and the number of zero crossings in the component must either equal or differ at most by one
- (ii) At any point, the mean value of the envelope defined by the local maxima and the envelope defined by local minima is zero.

A sifting process proposed to extract IMFs from the signal process the signal iteratively in order to obtain a component which satisfies above mentioned conditions. An intention behind application of these constraints on the decomposed components was to obtain a symmetrical mono-frequency component to guarantee a well-behaved Hilbert transform. It is shown that the Hilbert transform behaves erratically if the original function is not symmetric with X-axis or there is sudden change in phase of the signal without crossing X-axis (Huang *et al*, 1998).

Although the IMFs are well behaved in their Hilbert Transform, it may not necessarily have any physical significance. For example, an impulse response of a simple linear damped oscillator, which is physically mono-component with a single frequency, may not be necessarily fit the definition of the IMF and envelope function as illustrated in the comparison study shown in Section 2.4. Moreover the empirical sifting process does not guarantee exact modal decomposition. The EMD method proposed in Huang *et al* (1996) may lead to mode mixture and the analyzing signal needs to pass through a bandpass filter before analysis by EMD method (Appendix A).

The sifting process separates the IMFs with decreasing order of frequency i.e it separates high frequency component first and decomposes the residue obtained after separating each IMF till a residue of nearly zero frequency content does not obtained. Till date, there is no mathematical formulation derived for EMD method and the studies done in order to analyze the behavior of this method in stochastic situations involving broadband noise shows that the method behaves a dyadic filter bank when applied to analyze a fractional Gaussian noise (Flandrin *et al*, 2003). In this sense, the sifting process in the EMD method may be viewed as an implicit wavelet analysis and the concept of the intrinsic mode function in the EMD method is parallel to the wavelet details in wavelet analysis.

The wavelet packet analysis of the signal also can be seen as a filter bank with adjustable time and frequency resolution. It results in symmetrical orthonormal components when a symmetrical orthogonal wavelet is used as a decomposition wavelet. As a signal can be decomposed into symmetrical orthonormal components with wavelet packet decomposition, they also guarantee well behaved Hilbert transform. These facts motivated to formulate a sifting process based on wavelet packet decomposition to analyze a non-stationary signal, and it may be used as a damage detection technique for structural health monitoring.

## 2. A WAVELET PACKET BASED SIFTING PROCESS

### 2.1 MATHEMATICAL BACKGROUND

This section briefly describes the mathematical theory behind the terminology used in the development of wavelet packet based sifting process.

#### 2.1.1 Wavelet Packet Transform

A wavelet packet is represented as a function,  $\psi_{j,k}^i$ , where 'i' is the modulation parameter, 'j' is the dilation parameter and 'k' is the translation parameter.

$$\psi_{j,k}^i(t) = 2^{-j/2} \psi^i(2^{-j}t - k) \quad (2.1)$$

Here  $i = 1, 2, \dots, j^n$  and 'n' is the level of decomposition in wavelet packet tree. The wavelet  $\psi^i$  is obtained by the following recursive relationships:

$$\psi^{2i}(t) = \frac{1}{\sqrt{2}} \sum_{k=-\infty}^{\infty} h(k) \psi^i\left(\frac{t}{2} - k\right) \quad (2.2)$$

$$\psi^{2i+1}(t) = \frac{1}{\sqrt{2}} \sum_{k=-\infty}^{\infty} g(k) \psi^i\left(\frac{t}{2} - k\right) \quad (2.3)$$

Here  $\psi^1(t)$  is called as a mother wavelet and the discrete filters  $h(k)$  and  $g(k)$  are quadrature mirror filters associated with the scaling function and the mother wavelet function (Daubechies, 1992).

The wavelet packet coefficients  $c_{j,k}^i$  corresponding to the signal  $f(t)$  can be obtained as,

$$c_{j,k}^i = \int_{-\infty}^{\infty} f(t) \psi_{j,k}^i(t) dt \quad (2.4)$$

provided the wavelet coefficients satisfy the orthogonality condition.

The wavelet packet component of the signal at a particular node can be obtained as

$$f_j^i(t) = \sum_{k=-\infty}^{\infty} c_{j,k}^i \psi_{j,k}^i(t) dt \quad (2.5)$$

After performing a wavelet packet decomposition up to  $j^{th}$  level, the original signal can be represented as a summation of all wavelet packet components at  $j^{th}$  level as shown in Equation 2.6

$$f(t) = \sum_{i=1}^{2^j} f_j^i(t) \quad (2.6)$$

### 2.1.2 Wavelet Packet Node Entropy and Entropy Index

The entropy ‘E’ is an additive cost function such that  $E(0)=0$ . The entropy indicates the amount of information stored in the signal i.e. higher the entropy, more is the information stored in the signal and vice-versa. There are various definitions of entropy in the literature (Coifman and Wickerhauser, 1992). Among them, two representative ones are used here i.e. the energy entropy and the Shannon entropy. The wavelet packet node energy entropy at a particular node ‘n’ in the wavelet packet tree of a signal is a special case of  $P=2$  of the P-norm entropy which is defined as

$$e_n = \sum_k |c_{j,k}^i|^P \quad (P \geq 1) \quad (2.7)$$

where  $c_{j,k}^i$  are the wavelet packet coefficients at particular node of wavelet packet tree. It was demonstrated that the wavelet packet node energy has more potential for use in signal classification as compared to the wavelet packet node coefficients alone (Yen and Lin 2000). The wavelet packet node energy represents energy stored in a particular frequency band and is mainly used to extract the dominant frequency components of the signal. The Shannon entropy is defined as

$$e_n = -\sum_k (c_{j,k}^i)^2 \log[(c_{j,k}^i)^2] \quad (2.8)$$

Note that one can define his/her own entropy function if necessary. Here the entropy index (EI) is defined as a difference between the number of zero crossings and the number of extrema in a component corresponding to a particular node of the wavelet packet tree as

$$E.I. = |No\_of\_zero\_cross - No\_of\_extrema| \quad (2.9)$$

Entropy index value greater than 1 indicates that the component has a potential to reveal more information about the signal and it needs to be decomposed further in order to obtain simple frequency components of the signal.

## 2.2 METHODOLOGY

The proposed wavelet based sifting process starts with interpolation of data with cubic spline interpolation. The interpolated data increases the time resolution of the signal which will in turn increase the regularity of the decomposed components. The cubic spline interpolation assures the conservation of signal data between sampled points without large oscillations.

The interpolated data is decomposed into different frequency components by using wavelet packet decomposition. A shape of the decomposed components by wavelet analysis depends on the shape of the mother wavelet used for decomposition. A symmetrical wavelet is preferred as a mother wavelet in the process to guarantee symmetrical and regular shaped decomposed components. Daubechies wavelet of higher order and discretized Meyer wavelet shows good symmetry and leads to symmetrical and regular shaped components.

In case of the binary wavelet packet tree, decomposition at level 'n' results in  $2^n$  components. This number may become very large at a higher decomposition level and necessitate increased computational efforts. An optimum decomposition of the signal can be obtained based on the conditions required to be an IMF. A particular node (N) is split into two nodes  $N_1$  and  $N_2$  if and only if the entropy index of the corresponding node is greater than 1 and thus the entropy of the wavelet packet decomposition is kept as least as possible. Other criteria such as the minimum number of zero crossings and the minimum peak value of components can also be applied to decompose only the potential components in the signal.

Once the decomposition is carried out, the mono-frequency components of the signal can be sifted out from the components corresponding to the terminal nodes of the wavelet packet tree. The percentage energy contribution of the component corresponding to each terminal node to the original signal is used as sifting criteria in order to identify the potential components of the signal. This is obtained by summing up the energy entropy corresponding to the terminal nodes of the wavelet packet tree of the signal decomposition in order to get total energy content and then calculating the percentage contribution of energy corresponding to each terminal node to the total energy. Higher the percentage energy contribution, more significant is the component. Note that the decomposition is unique if the mother wavelet in the wavelet packet analysis is given and the sifting criteria are specified.

### **2.3 VALIDATION OF THE WAVELET PACKET BASED SIFTING PROCESS**

This section validates the proposed wavelet packet based sifting process by analyzing an acceleration response of a three storied structure. A simulation model consisting a linear

3 degree of freedom (DOF) spring-mass-damper system has been used for this purpose and the results have been compared to the analytical results as well as to the results obtained by Empirical Mode Decomposition method.

### 2.3.1 Simulation Model

A linear 3 DOF spring-mass-damper system used to validate a wavelet packet based sifting process is shown in Figure 2.1.

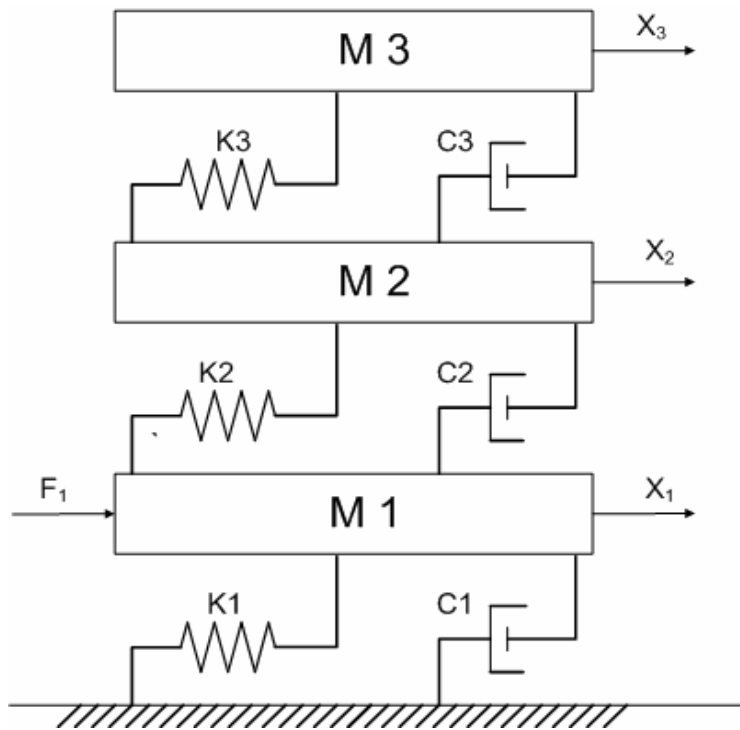


**Figure 2.1 3DOF mass-spring-damper system used in the simulation study**

The three storied structure is modeled as 3 lumped masses ‘ $M_1$ ,  $M_2$  and  $M_3$ ’ and the ground connected with each other by springs of stiffness ‘ $K_1$ ,  $K_2$  and  $K_3$ ’ and viscous dampers ‘ $C_1$ ,  $C_2$  and  $C_3$ ’. The structure is excited by applying a forcing function  $F_1$  at mass  $M_1$  which results in displacement of masses  $M_1$ ,  $M_2$  and  $M_3$  denoted by  $X_1$ ,  $X_2$  and  $X_3$  respectively.

The equations of motion of this structure in a matrix form can be written as

$$M\ddot{X}(t) + C\dot{X}(t) + KX(t) = F(t) \quad (2.10)$$

Here  $M$ ,  $C$  and  $K$  are mass, damping and stiffness matrices of the structure, respectively where

$$M = \begin{pmatrix} M_1 & 0 & 0 \\ 0 & M_2 & 0 \\ 0 & 0 & M_3 \end{pmatrix}, K = \begin{pmatrix} K_1 + K_2 & -K_2 & 0 \\ -K_2 & K_2 + K_3 & -K_3 \\ 0 & -K_3 & K_3 \end{pmatrix}, C = \begin{pmatrix} C_1 + C_1 & -C_2 & 0 \\ -C_2 & C_2 + C_3 & -C_3 \\ 0 & -C_3 & C_3 \end{pmatrix}$$

A subscript indicates mass number. In Equation 2.10,  $F(t)$  is a force function matrix whereas  $X(t)$ ,  $\dot{X}(t)$  and  $\ddot{X}(t)$  are displacement, velocity and acceleration response matrices where

$$\ddot{X}(t) = \begin{pmatrix} \ddot{X}_1(t) \\ \ddot{X}_2(t) \\ \ddot{X}_3(t) \end{pmatrix}, \dot{X}(t) = \begin{pmatrix} \dot{X}_1(t) \\ \dot{X}_2(t) \\ \dot{X}_3(t) \end{pmatrix}, X(t) = \begin{pmatrix} X_1(t) \\ X_2(t) \\ X_3(t) \end{pmatrix}, F(t) = \begin{pmatrix} F_1(t) \\ F_2(t) \\ F_3(t) \end{pmatrix}$$

This system of linear ordinary differential equations (ODE) can be solved analytically or numerically in order to get a response of the structure at every mass when subjected to an excitation force  $F(t)$ . Various ODE solvers, such as ‘ode23s’, are available in the commercial software ‘*MATLAB*’ to solve a system of linear ODEs.

### 2.3.2 Model Parameters

The values of structural parameters i.e. mass, stiffness of each element chosen for this study are

$$M_1 = M_2 = M_3 = 300kg$$

$$K_1 = K_2 = K_3 = 100,000N/m$$

The system damping is represented by a Rayleigh damping matrix proportional to the stiffness matrix. To demonstrate the basic concepts, zero damping is assumed here

without loss of generality i.e. value of proportionality factor is zero. The system natural frequencies are 1.29, 3.62 and 5.23 Hz. An impact force of intensity 1000 N is applied at first mass ( $M_1$ ) to excite the structure and the dynamic response data is numerically simulated by subroutines in the commercial software MATLAB. The data is sampled at a rate of 100Hz in order to simulate a data collected from an ordinary accelerometer.

### **2.3.3 Validation**

Acceleration response signal at the second mass element ' $\ddot{X}_2(t)$ ' is selected to illustrate the concept and accuracy of the proposed approach. The time resolution of the acceleration signal is increased by using a spline interpolation for interpolating the signal data with finer increment of 0.0005sec from 0.01sec. Wavelet 'DB36' is used as the analyzing mother wavelet to carry out a wavelet packet decomposition and by applying the proposed wavelet packet based sifting process in Section 2.1, the second floor acceleration signal is decomposed into three dominant components corresponding to three modes of the system as shown in Figure 2.2.

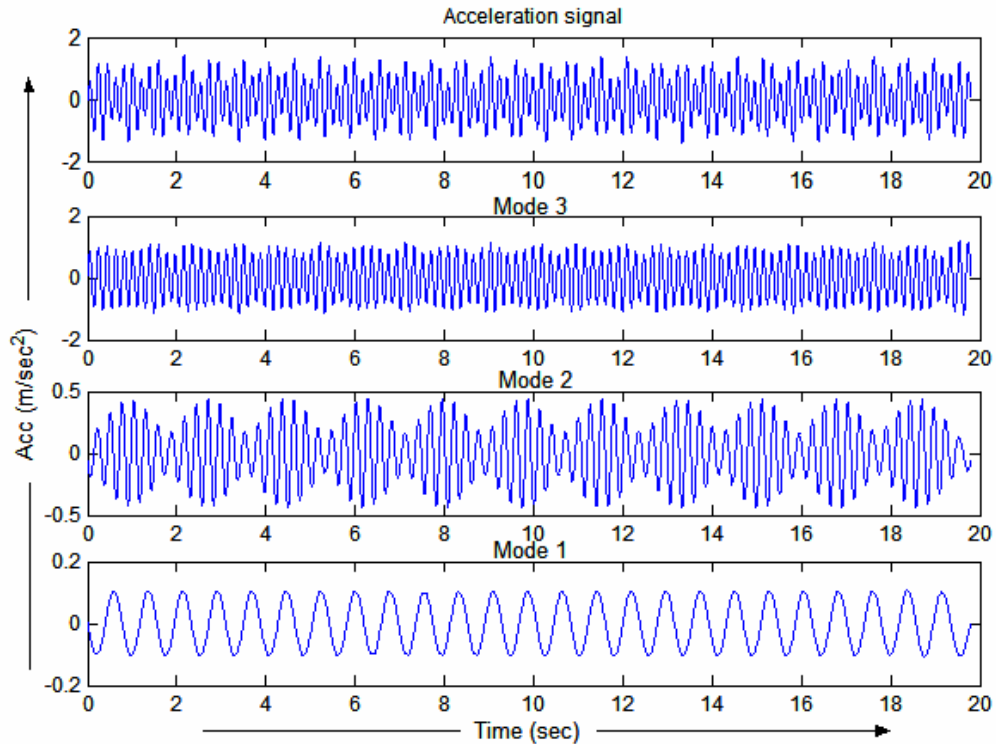


**Figure 2.2 Decomposition of an acceleration response signal of a linear 3DOF system by the proposed wavelet-packet sifting process.**

The top plot is the second floor acceleration signal whereas the bottom three plots are its dominant components sifted by the proposed approach.

The energy contribution of individual decomposed component is used to sift out the modal components of the signal. Table 2.1 shows the percentage energy contribution of the sifted dominant frequency components to the original acceleration signal at  $M_2$  and it illustrates that by evaluating the percentage energy contribution of the decomposed components, potential components of the signal thus can be sifted out.

**Table 2.1 Percentage Energy Contribution**

| Mode No. | Wavelet Packet Node No. | Percentage Contribution of Energy in Wavelet Packet Tree (%) |
|----------|-------------------------|--|
| 1        | (9,0)                   | 4.19   |
| 2        | (9,1)                   | 10.00  |
| 3        | (8,1)                   | 83.82  |

The wavelet packet node number in Table 2.1 is denoted as (x,y) where ‘x’ stands for a level of decomposition and ‘y’ stands for a position of the node at level ‘x’ when counted from left to right of the level and starting from ‘0’ in a wavelet packet tree.

In order to check accuracy of the sifting process, frequency content in the dominant components as well as the original signal is compared by calculating the Fourier transform of respective components. Figure 2.3 shows Fourier spectra of the components and the original signal. The peak frequencies observed in the Fourier spectra of the components, as shown in the Figure 2.3 are almost equal to the natural frequencies of the system calculated analytically. This shows that the proposed sifting process successfully sifted out modal components present in the acceleration response of the structure.

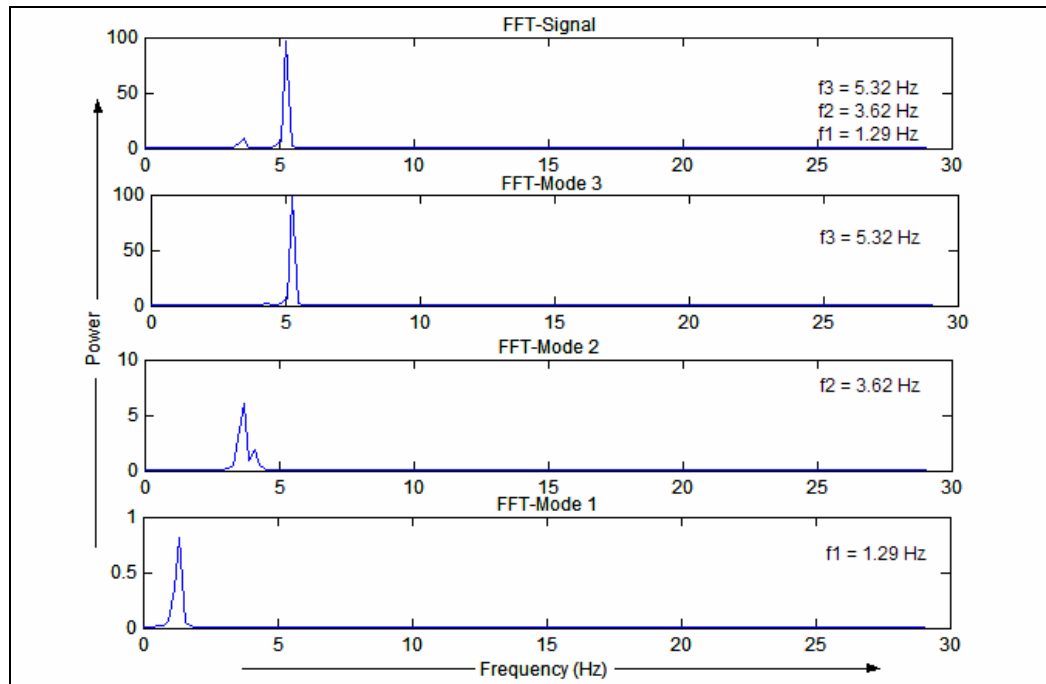
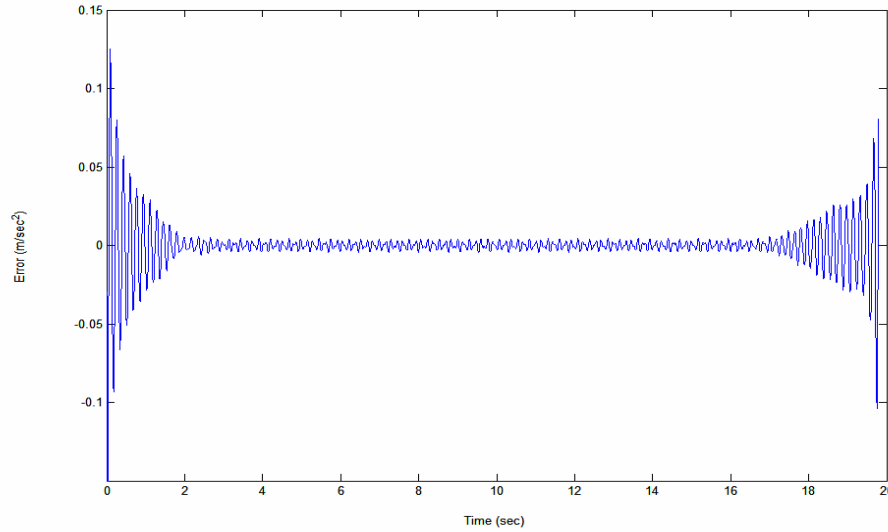


Figure 2.3 Fourier spectra of the original signal and its decomposed components

In order to check the completeness of the sifting process, the original signal is reconstructed by adding the three sifted components. Figure 2.4 shows very small error between reconstructed signal and original signal over a period of time.



**Figure 2.4 Error between the Reconstructed Signal and the Original Signal**

Error at the start and end of the signal is about  $0.1 \text{ m/sec}^2$  which decrease rapidly to the order of  $0.01 \text{ m/sec}^2$  and it is less than 1% of the original signal amplitude. The relatively greater values at the start and the end region of the signal may be attributed to the well-known end effects observed in wavelet analysis.

The results obtained from the proposed sifting process are compared with the results obtained by applying EMD method. Figure 2.5 shows the comparison results of these two methods when applied to the acceleration signal data from second mass of the linear undamped 3DOF structure. Exact modal responses obtained by carrying out classical modal analysis are also plotted as a benchmark in Figure 2.5.

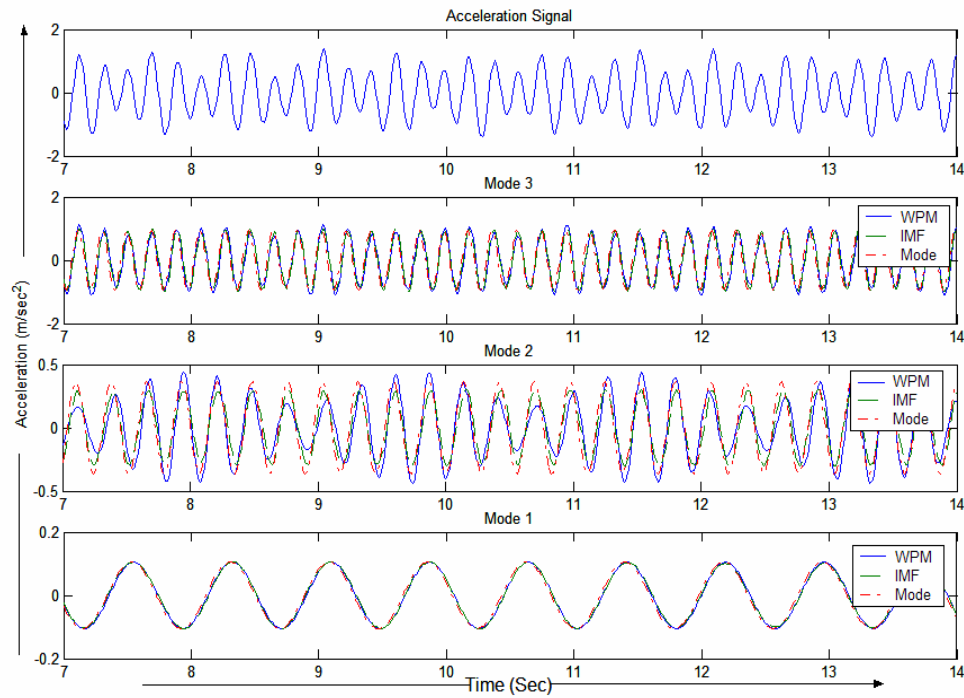


**Figure 2.5 Comparison of modal responses obtained from wavelet packet sifting process with the results obtained by EMD method and modal analysis**

As seen in Figure 2.5, there are no significant differences between the results obtained from the EMD method and the proposed sifting process. In case of first and third component, results obtained from all three methods are exactly same whereas in case of the second component, there are slight differences between the results obtained from all three methods. Note here that the results are shown for a short time span for zoom-in clarity and same results are observed for rest of the time span.

## **2.4 COMPARISON OF EMD METHOD AND WAVELET PACKET SIFTING PROCESS**

As seen in the previous section, a wavelet packet sifting process shows comparable results as given by EMD method. In order to further explore the effectiveness of the proposed sifting method, the method is applied for different test signals and the results

are compared with the those obtained with the EMD method. The similarities and differences between the EMD method and the proposed wavelet packet sifting process are studied by applying these methods for two test signals: (1) a linear chirp signal, (2) the impulse response of a linear single degree of a freedom spring-mass-damper system.

A linear chirp signal, also called as sweeping frequency signal, is a sinusoidal signal whose frequency is zero at start of the signal and increases linearly till the end. The chirp signal used for testing is of amplitude 2 units with a sample rate of 100 Hz that starts at DC (??) and reaches linearly to 31Hz in 19.75 sec. Both of the methods give same results as shown in Figure 2.6 and Figure 2.7.

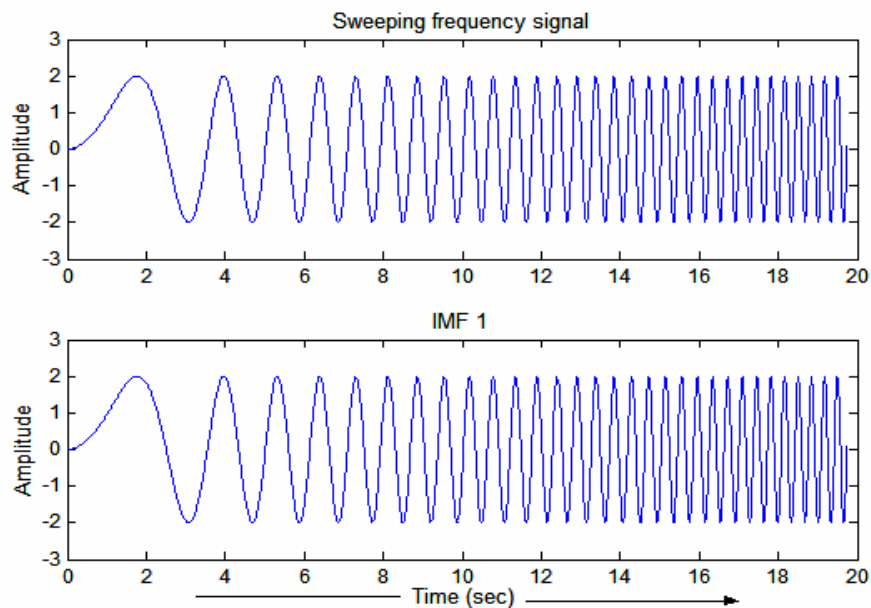


**Figure 2.6 Decomposition of a chirp signal by the EMD method**

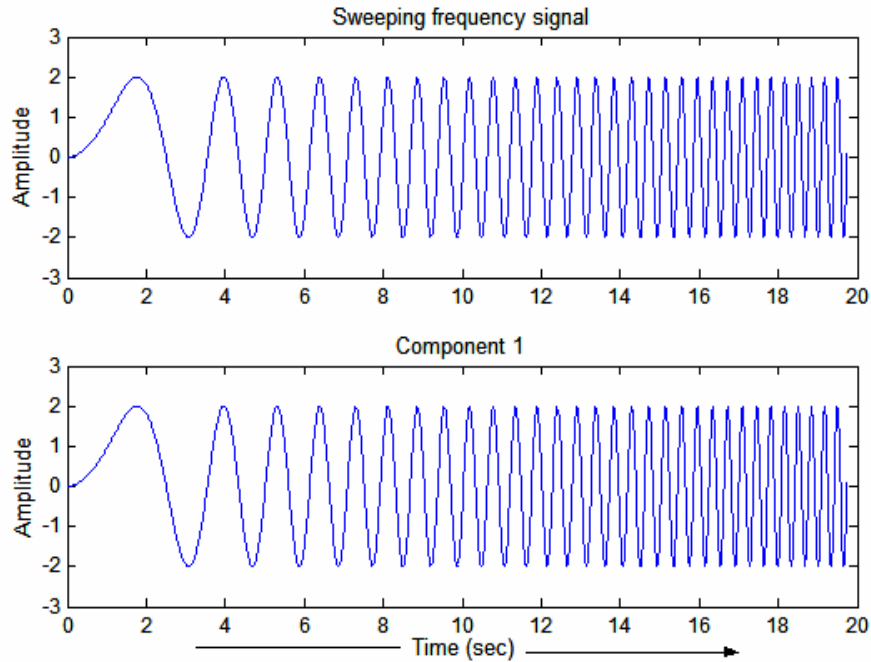
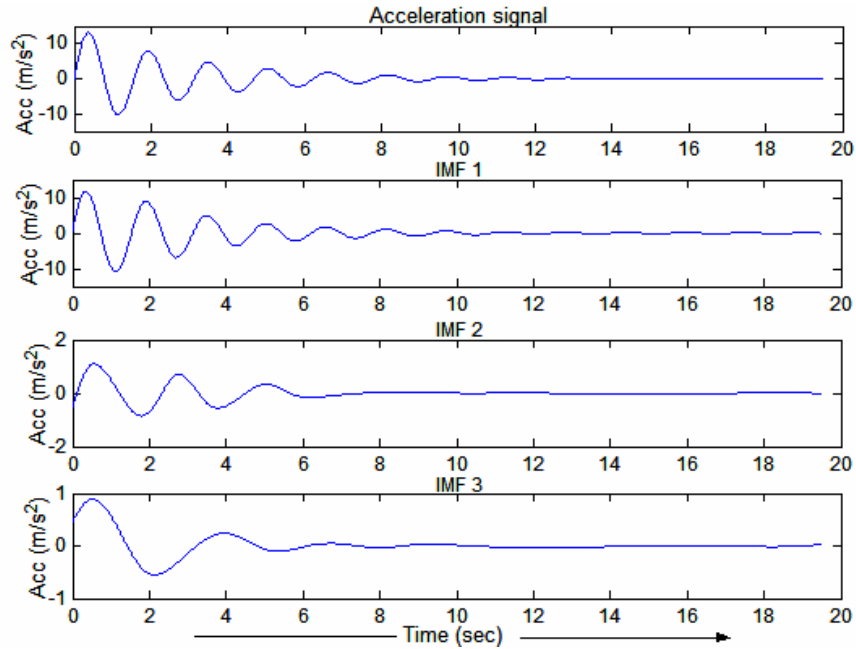


**Figure 2.7 Decomposition of a chirp signal by the propose sifting process**

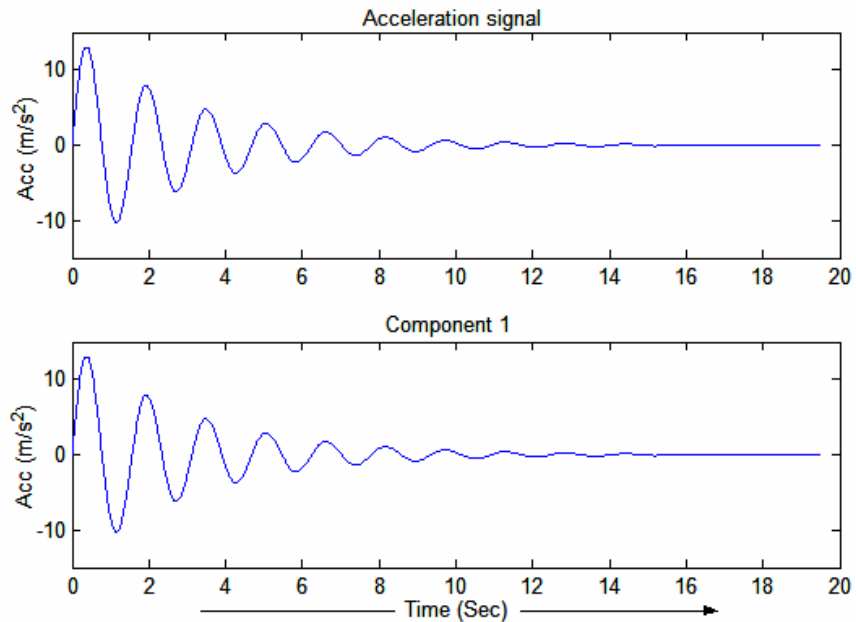
In case of the EMD method, the chirp signal already satisfies the conditions necessary to be an IMF and therefore does not decompose further resulting in single component decomposition as shown in Figure 2.6. In case of wavelet packet sifting process, the original signal already satisfies the stopping criteria of the proposed sifting process i.e. the value of entropy index is less than 1 here and thus does not decompose further resulting in single component as shown in Figure 2.7.

Figure 2.8 shows the decomposition results obtained by the EMD method for the acceleration response from a linear SDOF damped system subjected to impact loading. The signal is physically a monocomponent having a frequency equal to the damped natural frequency of the system. However, this acceleration signal does not fit in a definition of the IMF due to existence of damping. The EMD method results into three IMFs having different frequency contents. In contrast to the EMD method, the proposed wavelet packet sifting process has resulted into only one single-frequency component

having its frequency equal to the damped natural frequency of the system, as shown in Figure 2.9.



**Figure 2.8** Decomposition of an impulse acceleration response signal of a SDOF linear damped system by the EMD method.



**Figure 2.9** Decomposition of an impulse acceleration response signal of a linear SDOF system by the proposed wavelet packet sifting process.

Thus the proposed wavelet packet based sifting process can decompose the signal into monocomponents and give meaning results. In the case of sweeping frequency signal, the proposed sifting process showed similar results as EMD method, whereas for a vibration response of SDOF system, it worked better than EMD method. Thus the proposed sifting process may serve as a better signal analysis method than the EMD method.

### 3. APPLICATION FOR STRUCTURAL HEALTH MONITORING

Structural health monitoring is defined as the process of detecting damage in a structural or mechanical system. Damage in a system causes a change in dynamic properties of a system which in turn affect the system modal parameters. Thus system modal parameters i.e. the natural frequency and mode shape can be monitored in order to detect the time and severity of damage. When a vibration signal is decomposed into its mono-components by the proposed wavelet packet sifting process, these components often represent modal responses associated with the system natural frequencies. The instantaneous modal parameters of the structure are defined in the following paragraph.

#### **Instantaneous Modal Parameters:**

The free vibration response of a time varying system can be decomposed into a number of instantaneous vibration modes having variable frequency content and a slow time varying amplitude. One of the limiting cases is when the system is time invariant where the decomposition results in the modal decomposition of the response. The concept of instantaneous natural frequency and normalized instantaneous mode shape is briefly described herein. The dynamics of a time-varying system can be described by:

$$[M(t)]\{\ddot{\mathbf{x}}\} + [C_d(t)]\{\dot{\mathbf{x}}\} + [K(t)]\{\mathbf{x}\} = \{\mathbf{F}\} \quad (3.1)$$

where  $\{\mathbf{x}\}$  is the response vector and  $\{\mathbf{F}\}$  is the vector of external excitation,  $[M(t)]$ ,  $[K(t)]$  and  $[C_d(t)]$  are the time-dependent mass, stiffness and damping matrices of the system, respectively. In the present study the free vibration response due to an impact loading is studied.

The system response can be written in a form similar to the modal decomposition for time invariant systems as:

$$\mathbf{x}(t) = \sum_{i=1}^N \mathbf{X}^{(i)}(t) A^{(i)}(t) \cos(\Phi^{(i)}(t)) \quad (3.2)$$

where  $\mathbf{X}^{(i)}(t)$ ,  $A^{(i)}(t)$ ,  $\Phi^{(i)}(t)$  are continuous functions of time. By applying similar analogy of the modal parameters in case of a time invariant system, we define instantaneous modal frequency and normalized instantaneous mode shape vector. Their expressions can be found in Equation 3.3 and 3.4.

$$\omega^{(i)}(t) = \frac{d}{dt}(\Phi^{(i)}(t)) \quad (3.3)$$

$$\mathbf{X}_{norm}^{(i)} = \left( \frac{\mathbf{X}^{(i)}}{X_p^{(i)}} \right) \quad (3.4)$$

Where  $\omega^{(i)}(t)$  is the instantaneous frequency of the  $i^{\text{th}}$  mode and  $\mathbf{X}_{norm}^{(i)}$  is the  $i^{\text{th}}$  normalized instantaneous mode shape. In case of a system without damage these parameters are constant over a period of time and correspond to the damped natural frequency and mode shape vector. A change in these instantaneous measures indicates change in system parameters which may be a result of structural damage. These parameters are monitored for the purpose of damage identification in the structure.

The application if the proposed approach is first evaluated for simulation data where different damage cases in different noise environment are considered, and in the later part of the section, the methodology is applied for damage detection by analyzing experimental data.

### **3.1 NUMERICAL STUDIES:**

In this study the same 3DOF structural model in Figure 2.1 is employed. A proportional damping is employed here and a damping matrix is proportional to the stiffness matrix with a proportionality factor of 0.0002. Structural damage is simulated by linearly reducing the stiffness of spring K2 up to certain extent. By selecting the rate of change in stiffness reduction, both cases of damage i.e. sudden stiffness loss and progressive stiffness degradation are simulated. Ideally sudden damage happens at a particular instant and stiffness of the structure decreases instantly at this moment. However, in a practical case, damage occurring in a fractions of second is considered as a sudden damage, therefore in the numerical simulation, a sudden damage is simulated by considering stiffness loss in a sufficiently small time period i.e. five time steps. For both cases, the proposed wavelet packet based sifting process is first applied to the simulated response data to sift out the dominant components and the Hilbert transform is then applied to investigate their transient frequency characteristics for the purpose of structural health monitoring.

The performance of the proposed approach in presence of measurement noise is evaluated for one of the cases by adding noise to all vibration acceleration responses. The measurement noise is simulated as a Gaussian white noise process with zero mean and RMS value of 5% of the RMS value of third floor acceleration signal. The 5% noise level is justified with the fact that in case of an earthquake excitation, as the ground acceleration is very high and the measuring instrumentation is very sturdy, the measurement noise is of a fairly low level in comparison to the measured signal.

### 3.1.1 Case Study 1: Detection of Sudden Damage

In the case study of detection of sudden damage, a sudden stiffness loss is introduced at  $t=15\text{sec}$  by linearly reducing stiffness of the middle spring, i.e.  $K_2$  by 10% in a short time interval from  $t=15\text{sec}$  to  $t=15.05\text{sec}$ . Damage in such a small time interval may be reasonably considered as *sudden*. In a practical application, measurement data are collected with certain sampling rate and so a sudden stiffness loss may be treated as linear reduction between two sampling points. Without loss of generality only the dominant component of acceleration response data of  $M_2$ , which is obtained by the proposed sifting process and corresponds to the highest mode of the healthy system, is selected for the analysis.

Figure 3.1 plots the component and the associated instantaneous frequency history; the latter was obtained by Hilbert transform. An exact solution for the instantaneous frequency is also presented for comparison. A sudden change in the instantaneous frequency can be observed at  $t=15\text{ sec}$ , implying some sudden damage has occurred at that moment. The amount of frequency drop provides a global measure of damage severity due to a local stiffness loss. Data analysis of other dominant components has lead to the similar conclusions. It should be pointed out that numerical differentiation of the phase curve of Hilbert transform of a signal may generally produce fluctuated instantaneous frequency history. The associated variance is reduced in this study by filtering the phase angle curve.

A normalized mode shapes at mass  $M_2$  and  $M_3$  associated with the highest frequency mode are shown in Figure 3.2. An exact solution for normalized mode shape is also shown as a dotted line in figure for comparison. The change in normalized mode

shape at  $t=15\text{sec}$  clearly indicates damage in the system.

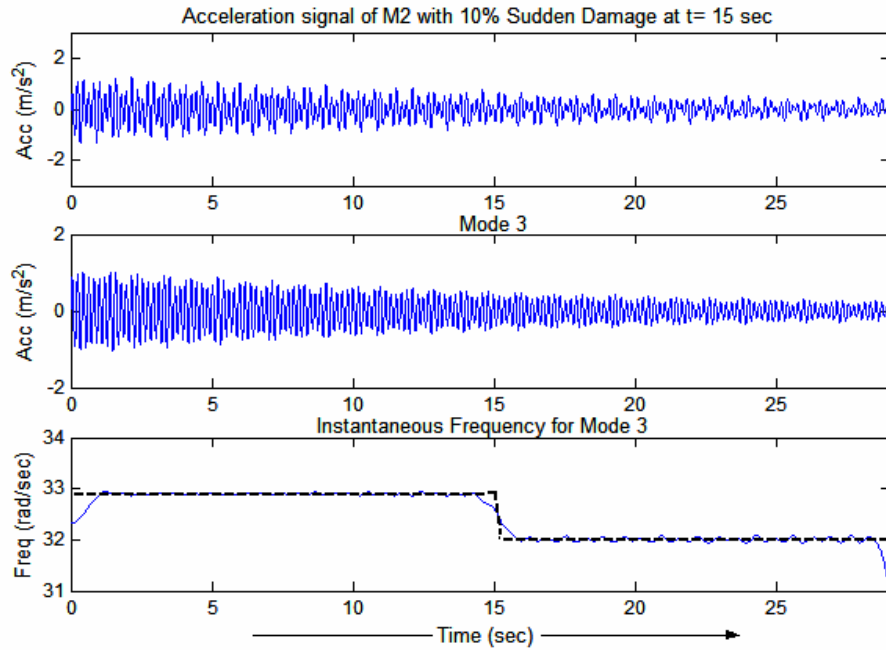


Figure 3.1 Results from a case study for sudden damage using a free vibration signal

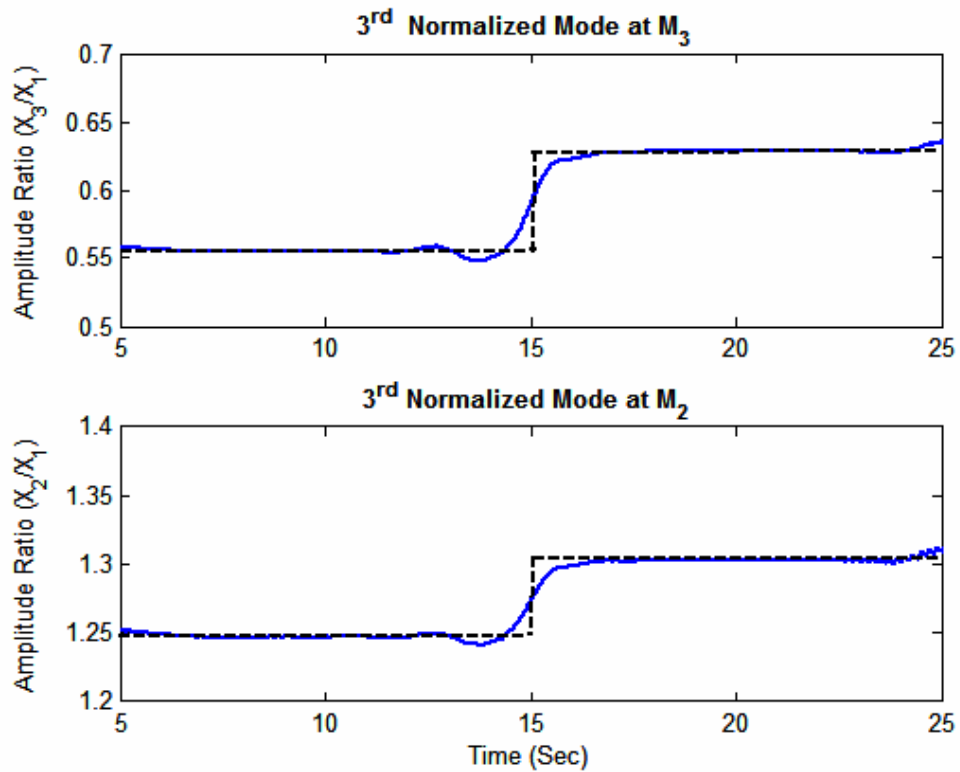


Figure 3.2 Instantaneous normalized 3<sup>rd</sup> mode shape at M2 and M3 indicating sudden damage at  $t = 15\text{sec}$

### 3.1.1.1 Effect of Measurement Noise:

The effects of measurement noise in the signal on results are evaluated by adding ‘5%’ random noise to the vibration response of each floor. The results obtained for instantaneous third mode frequency and normalized mode shape are shown in Figure 3.3 and Figure 3.4 respectively. It can be observed that while the results obtained for instantaneous natural frequency remains unaffected, the mode shape results get affected. This is evident, as the normalized mode shape is calculated as a ratio of amplitudes of two signals and with the presence of noise, the results get deteriorated. Moreover, the SNR is smaller in the later part of the signal, which reflects in the deviation of results from corresponding theoretical values.

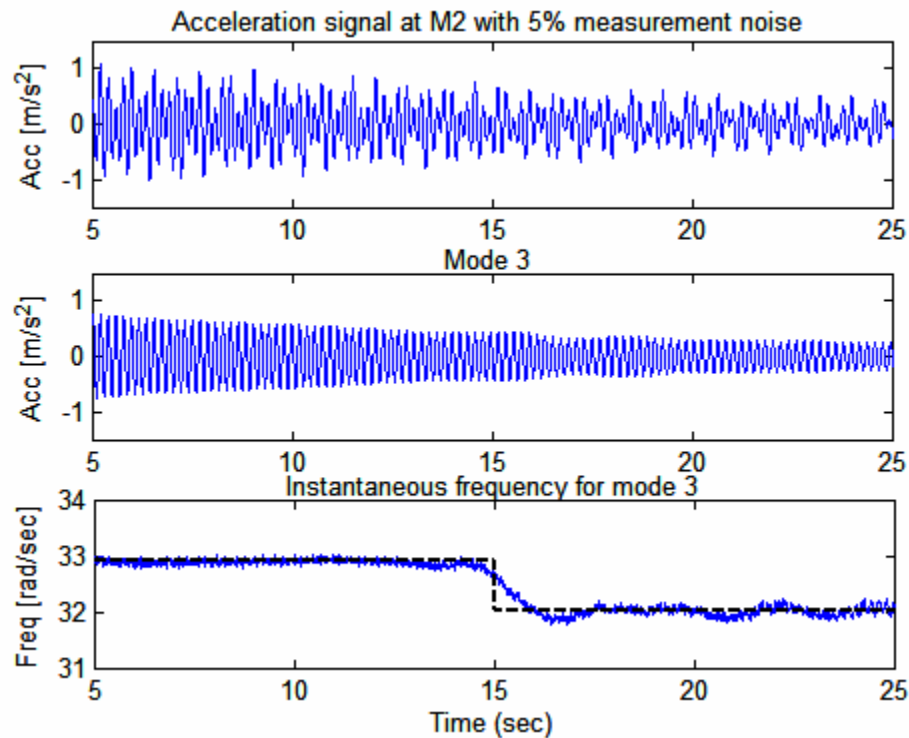
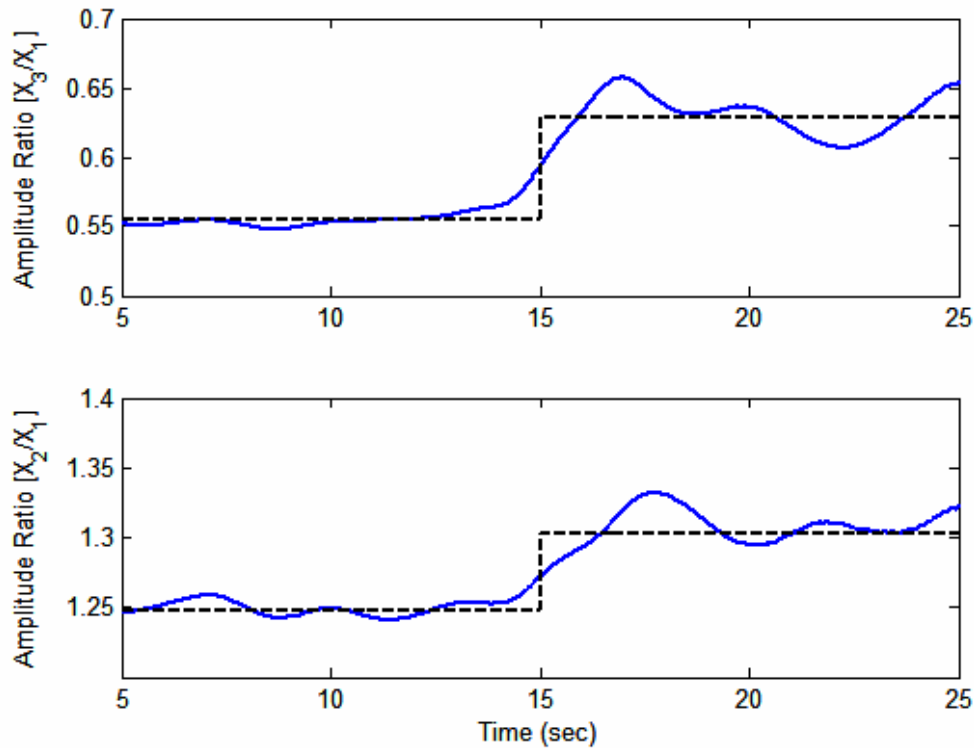


Figure 3.3 Sudden damage detection in presence of measurement noise



**Figure 3.4 Instantaneous normalized 3<sup>rd</sup> mode shapes at M2 and M3  
In presence of measurement noise**

### ***3.1.1.2 Forced Vibration Response:***

Effectiveness of the proposed sifting process for damage detection is also examined for the same 3DOF spring-mass-damper system subjected to a harmonic force with the frequency of 2.4 Hz. To simulate the real-life conditions, measurement noise with a standard deviation of  $0.03 \text{ m/sec}^2$  is added to the acceleration signal shown in Figure 3.5. A sudden damage is introduced in the system by linearly reducing the stiffness of second spring ( $K_2$ ) by 20% in a time interval of 15 -15.05 sec. The highest contributed mode, shown in Figure 3.5, is separated from the signal by applying the proposed wavelet packet based sifting process. The transient frequency of this component is calculated with the help of Hilbert transform of the sifted component.

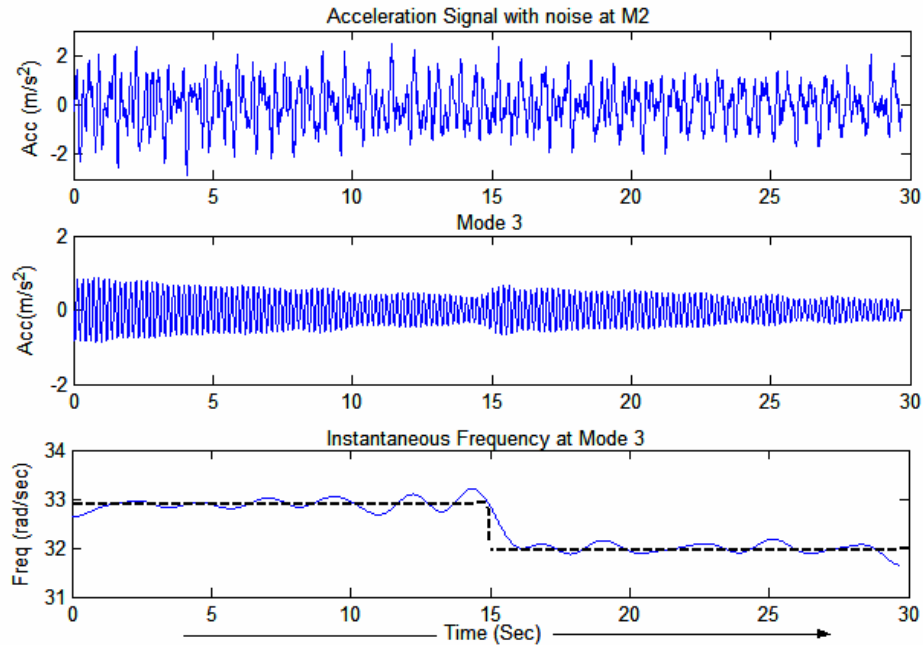


**Figure 3.5 Sudden damage detection using a forced vibration signal with random noise of 0.03 standard deviation.**

It can be observed in Figure 3.5 that the associated instantaneous frequency is reduced permanently at  $t = 15\text{sec}$  indicating an occurrence of the damage in the system. It should be pointed out that in order to use a forced vibration signal for health monitoring, information of the corresponding healthy system or measurement data of loading history may be needed for reference. For this lightly contaminated signal, the proposed approach provides a good result for damage detection. It is expected that the clarity of the damage detection will decrease for a higher-level measurement noise and a smaller stiffness loss. Noise effects on effectiveness of the proposed approach are further investigated in Section 4.2.

### ***3.1.1.3 Effect of Damage Severity:***

Figures 3.6 and 3.7 provide a comparison of the instantaneous frequency and the instantaneous mode shapes of the system for three different levels of damage, i.e. 5%, 10%, and 15% sudden local stiffness loss of K2, respectively, at  $t = 15$  seconds.

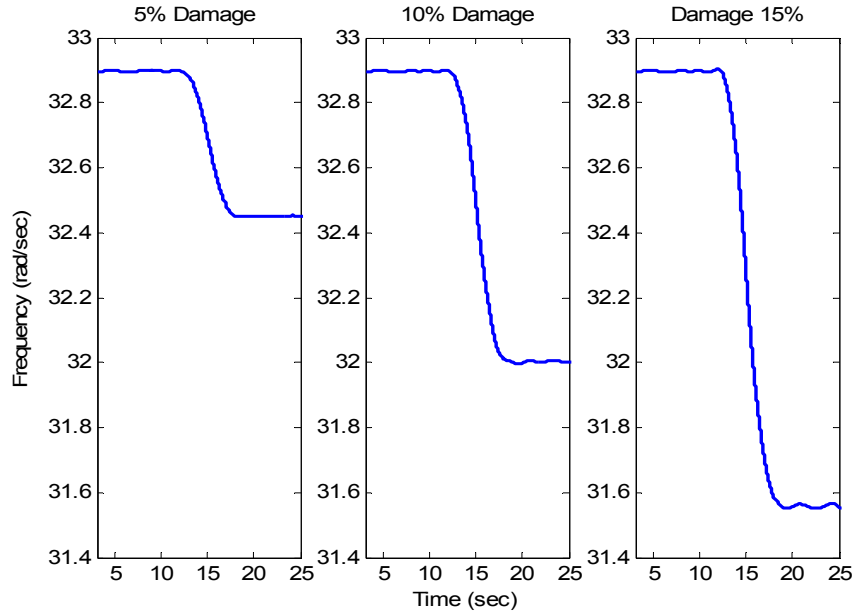


**Figure 3.6 Comparison of instantaneous frequency of 3<sup>rd</sup> mode for detection of damage of 5%, 10%, and 15% sudden stiffness loss of K2.**

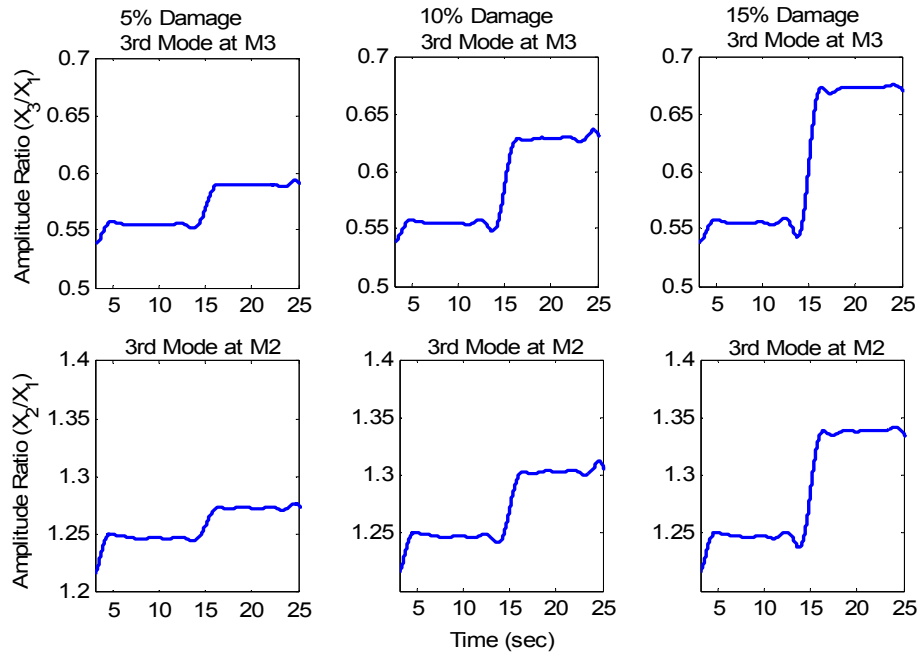


**Figure 3.7 Comparison of normalized instantaneous modal shapes of the 3<sup>rd</sup> mode for detection of damage of 5%, 10%, and 15% sudden stiffness loss of K2.**

The results in Figure 3.6 present change in the damped natural frequency of the highest mode, obtained by sifting the acceleration response of M2. In all three cases, the sudden

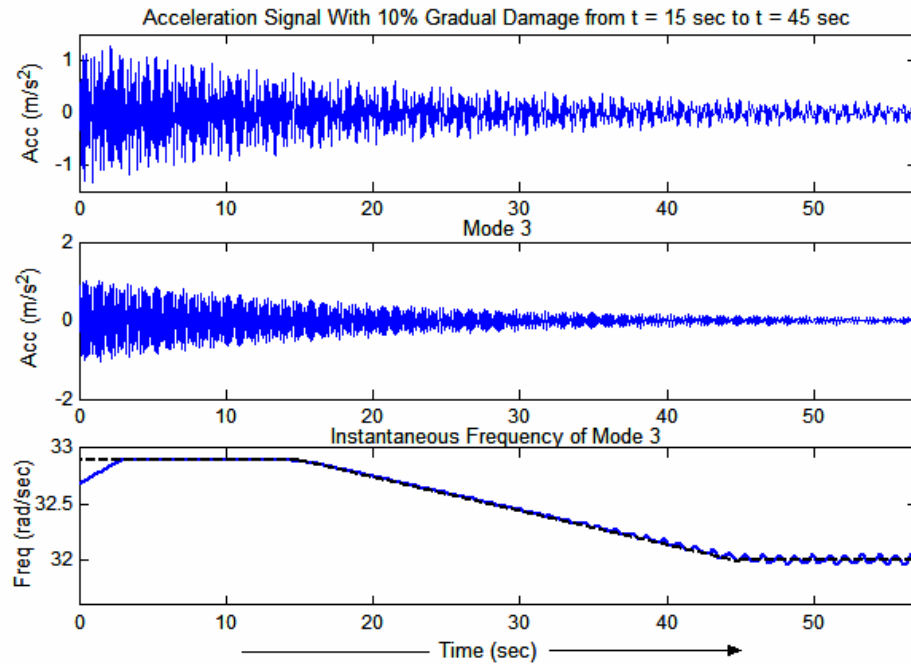
damage can be clearly identified by sudden changes of these instantaneous frequencies. Note that the 5%, 10%, and 15% stiffness of K2 cause 1.4%, 2.8%, and 4.1% reduction in frequency, respectively. In general, more severe damage is easier to detect. It is expected that the abrupt change in the instantaneous frequency becomes less and less recognized for smaller local stiffness loss.

Figure 3.7 shows the normalized modal shape of the highest mode. Note that the absolute values of the amplitude ratio of M2 and M3 with respect to M1 are used for convenience. Sudden damage at  $t=15$  seconds are successfully detected. The 5%, 10%, and 15% stiffness losses of K2 result in 7.3%, 14.5%, and 21.6% change in the modal shape, respectively. In general, the instantaneous modal shape is more sensitive to a small local stiffness loss. It can be shown that a local stiffness loss is of order of  $\epsilon$  may result in change in the natural frequency of order  $\epsilon^2$  and change in the modal shape of order  $\epsilon$ . Therefore, the modal shape is a more sensitive index for structural damage. However, measurement data at multiple locations must be available if the instantaneous modal shape is to be traced.

### **3.1.2 Case Study 2: Detection of Progressive Damage**

To model a progressive stiffness degradation, the value of K2 is reduced linearly by 10% from  $t=15$ sec to  $t=45$ sec. The acceleration signal from the middle mass is selected for analysis, as shown in upper part of the Figure 3.8. The highest-mode component of the signal obtained by the proposed sifting process and the associated instantaneous frequency are shown in the middle and bottom parts respectively of Figure 3.8. A gradual change in the instantaneous frequency is clearly observed in the same time interval as specified for the progressive damage in the data simulation. The trend and

amount of change in instantaneous frequency provide valuable information as how stiffness degradation is developed. Note that despite of the same trend, the change in the instantaneous frequency in Figure 3.8 is not linear.



**Figure 3.8 Results from a case study for Monitoring Progressive Damage**

The results for instantaneous 3<sup>rd</sup> mode shape at  $M_2$  and  $M_3$  normalized with respect to  $M_1$  are shown in Figure 3.9. It can be observed that the normalized mode shape follows the same trend as of stiffness and the nature of damage can be estimated with this method.

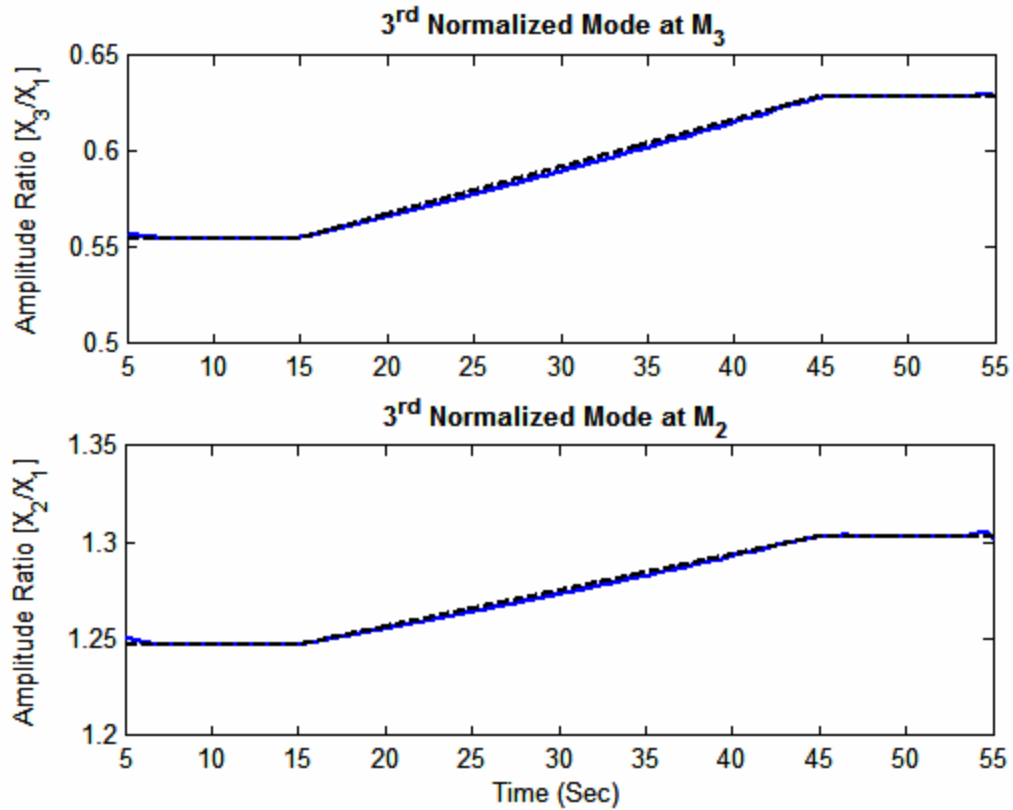


Figure 3.9 Normalized 3<sup>rd</sup> mode shape results for monitoring progressive damage

## 3.2 EXPERIMENTAL VALIDATION

From the damage detection results obtained in numerical studies, it is seen that by incorporating wavelet packet sifting process with Hilbert Transform, sudden as well as gradual damage can be successfully identified. In order to evaluate the potential of the methodology in practical applications, the methodology is applied for experimental data obtained in a shaking table test, described below.

### 3.2.1 Shaking Table Test

The shaking table test was performed at the Disaster Prevention Research Institute (DPRI), Kyoto University, Japan. In the test, a two-storey full-size wooden frame, shown

in Figure 3.10 was excited by the NS component of 1940 El Centro earthquake and the acceleration signal data was collected at each floor of the structure.



**Figure 3.10 Two-story wooden structure (left) and observed damage (right)**

The test was characterized by several test runs and at each test run the structure was excited with a normalized ground excitation targeted at a definite intensity in increasing order. The test was carried out until the structure lost its load carrying capacity. The structure was excited at increasing load levels of  $1 \text{ m/s}^2$ ,  $1.5 \text{ m/s}^2$ ,  $2 \text{ m/s}^2$ ,  $2.5 \text{ m/s}^2$ ,  $3 \text{ m/s}^2$ ,  $3.5 \text{ m/s}^2$ ,  $4 \text{ m/s}^2$ ,  $6 \text{ m/s}^2$  and  $8 \text{ m/s}^2$ . Various types of damages were observed in the structure at different load levels. A detailed description about the test can be found in Shimizu et al (2001) and Hou (2001).

### **3.2.2 Methodology**

As mentioned earlier, in order to identify the natural frequency and mode shape, it is necessary to sift out, from the measured response data, a component signal that corresponds to the vibration mode of interest. This can be accurately done in the case of a free vibration response, since each modal response can be described as a signal with mono-frequency content. Thus the modal components can be completely sifted out and

the instantaneous natural frequency and normalized mode shape can be accurately identified and monitored for SHM (Hera et al., 2004).

However, when a structure is subjected to a non-stationary excitation, e.g. earthquake excitation, the separation of each modal component in the vibration response is not as evident as in case of free vibration response. Moreover, if some damage happened in the system during this excitation period, due to the time varying structural properties, the classical Fourier transform based deconvolution technique can not be applied to deconvolve the impulse response from the vibration response. This fact rules out the possibility of obtaining impulse response of a structure to accurately calculate the instantaneous modal parameters. However, in case of a structure subjected to a seismic excitation, the energy in the vibration response is concentrated in frequency bands corresponding to the instantaneous natural frequencies of the structure. This property is further used to sift out the signals of interest by a wavelet packet sifting (WPS) technique.

The methodology can be illustrated in a better way by representing the signal energy in time-scale (frequency) domain. The signal energy is graphically shown with help of the CWT maps. Details regarding CWT can be found in (Mallat, 1999) or any other reference on the wavelet transform.

Without loss of generalization, the methodology is explained for a linear 3DOF system sketched in Figure 2.1, subjected to the El-Centro earthquake excitation. The structural response is simulated for a case of no stiffness loss. The CWT map of the excitation is presented in Figure 3.11, whereas Figure 3.12 shows the CWT map of the acceleration response (with respect to ground) at location M1. It can be observed that the energy is concentrated in the frequency bands corresponding to the natural frequencies of

the structure. Thus the natural frequency of the components corresponding to these frequency bands can be monitored to assess structural health.

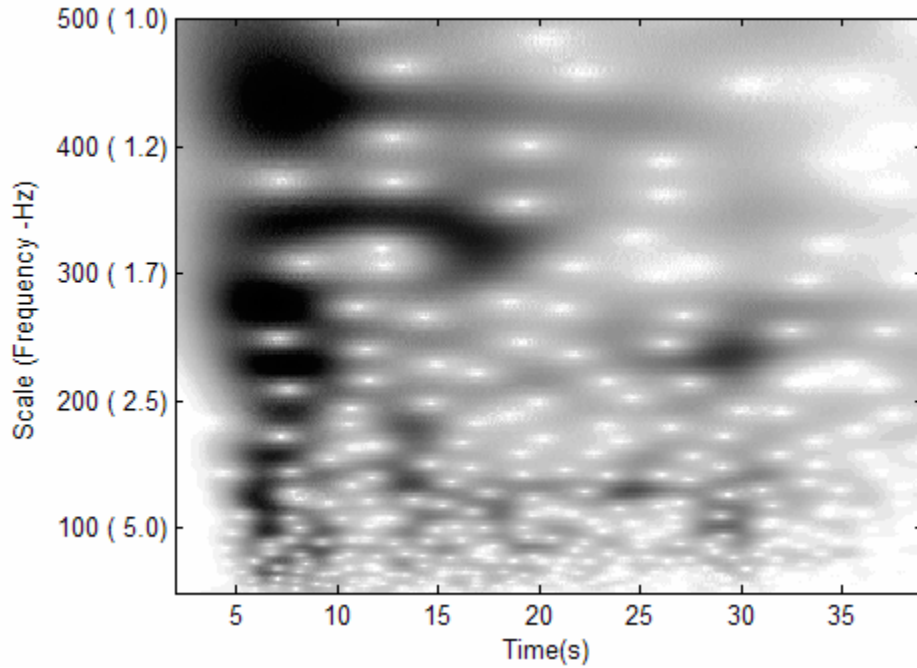


Figure 3.11 CWT map of the El Centro earthquake signal.

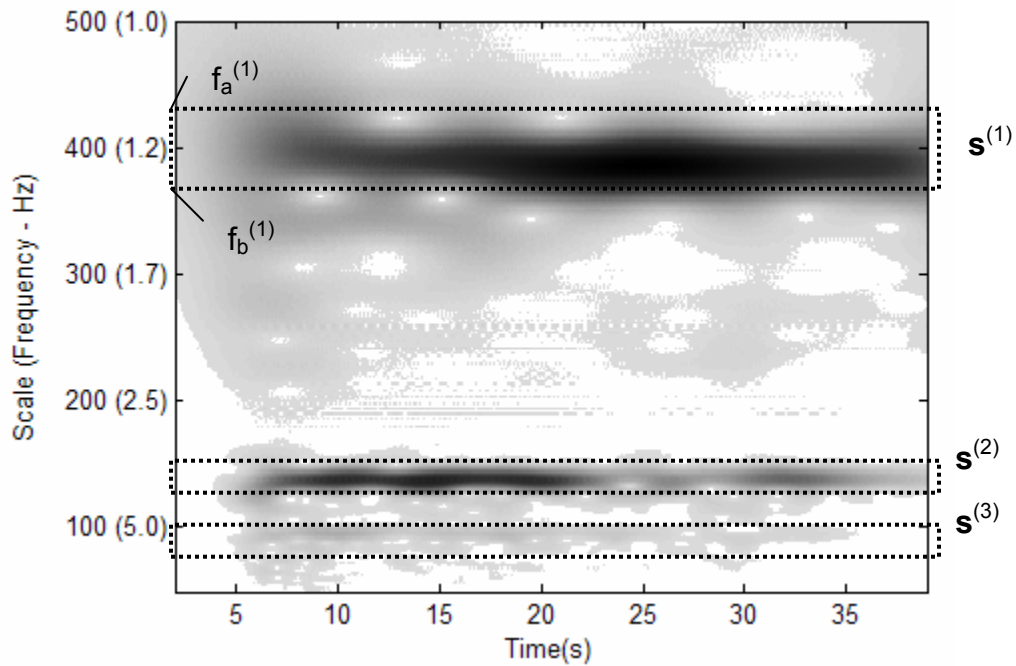


Figure 3.12 CWT map of the acceleration response measured at M1.

The proposed methodology is applied for a set of experimental data obtained by a shaking table test.

### 3.2.3 Results for Experimental Data and Discussion

The acceleration signal data at nominal load levels of  $1\text{m/s}^2$ ,  $2\text{m/s}^2$ ,  $3\text{m/s}^2$ ,  $4\text{m/s}^2$ ,  $6\text{m/s}^2$  and  $8\text{m/s}^2$  are considered in this study. The acceleration signals at first floor as well as the corresponding excitation signal at the base were decomposed by using the wavelet packet sifting process. Db36 was used as an analyzing wavelet because of its regularity and symmetrical properties. By implementing the methodology described in section 3, the fundamental frequency component was sifted out from the acceleration signal collected from the accelerometer mounted on the first floor. The node corresponding to the fundamental frequency component in the wavelet packet tree can be easily identified by comparing the energy contribution associated with that node and the corresponding node of excitation signal wavelet packet tree. The percentage energy contribution of fundamental frequency component in the excitation and structural response wavelet packet trees for different load levels is shown in Table 3.1.

**Table 3.1. Percentage Energy Contribution at Various Load Levels**

| Signal No. | Load Level<br>( $\text{m/s}^2$ ) | Wavelet Packet<br>Node No. | Percentage Contribution of Energy in<br>Wavelet Packet Tree (%) |                    |
|------------|----------------------------------|----------------------------|---|--------------------|
|            |                                  |                            | Excitation Signal   | First Floor Signal |
| 1          | 1                                | (11,2)                     | 12.10   | 50.57              |
| 2          | 2                                | (12,7)                     | 3.60  | 27.87              |
| 3          | 3                                | (13,12)                    | 7.39  | 31.59              |
| 4          | 4                                | (12,2)                     | 7.05  | 35.37              |
| 5          | 6                                | (13,6)                     | 3.71  | 40.15              |
| 6          | 8                                | (13,2)                     | 1.16  | 19.85              |

The wavelet packet node number is denoted as (m,n) where 'm' is a level of decomposition and 'n' is a node number at level 'm' in the wavelet packet tree when counting from left to right. Table 3.1 clearly demonstrates that the percentage energy contribution of the lowest fundamental frequency component to the acceleration response in its wavelet packet tree is significantly larger than the percentage energy contribution to the excitation signal of the component corresponding to the same node number in the wavelet packet tree of the excitation signal. Thus the lowest natural frequency component in the acceleration response can be easily identified by calculating and comparing the percentage energy contribution of decomposed components of both signals. The excitation signal, the corresponding acceleration response signal of the first floor, and the sifted component with the fundamental frequency for the first floor response for a load level of  $1\text{m/s}^2$  is shown in Figure 3.13.

Similar test results are obtained for rest of the load levels. The phase angle curve for corresponding fundamental frequency components can be computed by taking the Hilbert transform of the components as described in the previous sections. The phase angle curve calculated for above listed load levels is shown in Figure 3.14. Note here that the phase angle variation at each load level is calculated over a 20 sec time interval from 5-25 sec as the signal strength is lower in rest of the part of a signal. For a presentation purpose, the origin of phase angle curve at each load is changed to match the last value for previous load level.

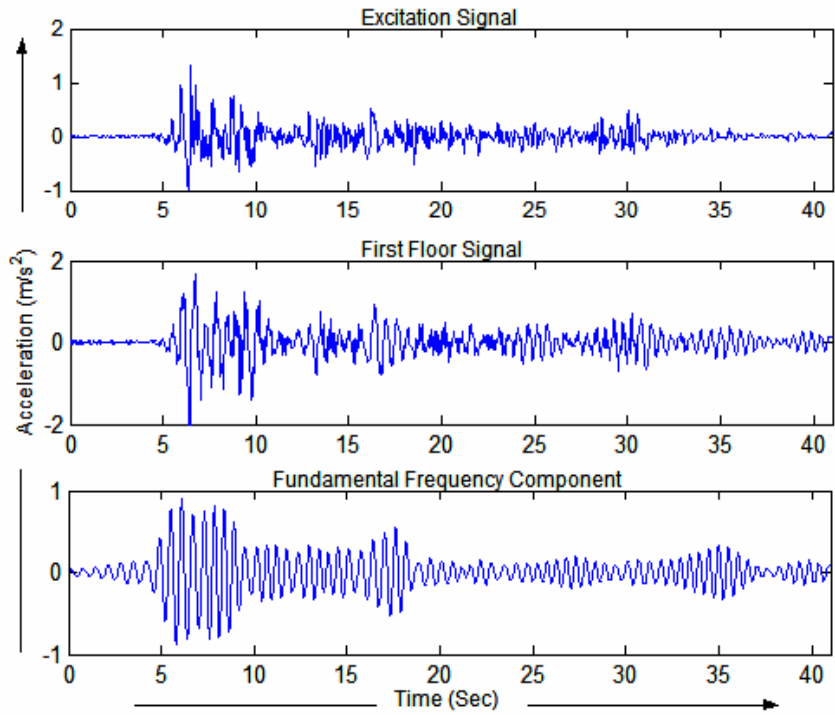


Figure 3.13 Excitation signal, first-floor acceleration signal and its natural frequency component at load level of  $1\text{m/s}^2$

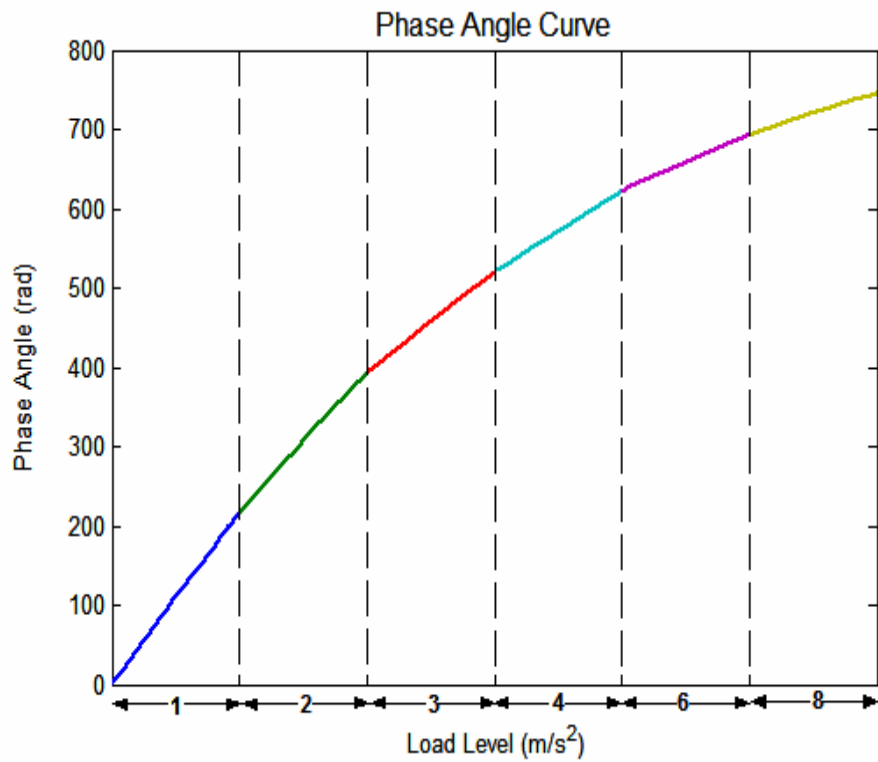
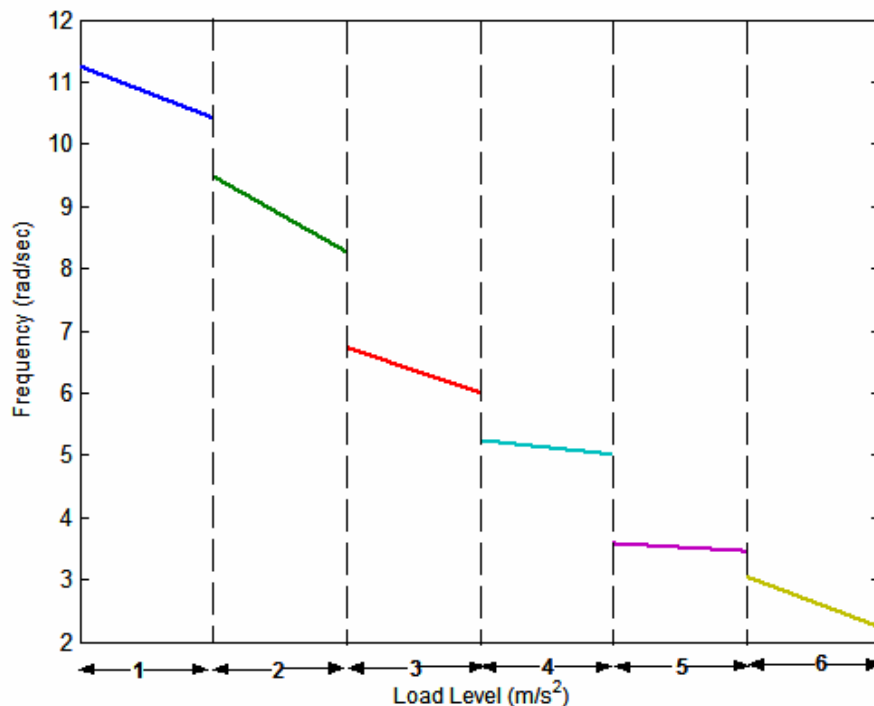


Figure 3.14 Phase angle variation at different load levels

The instantaneous frequency at each load level can be calculated by carrying out a numerical differentiation of the phase angle curve with respect to time. A direct numerical differentiation of the phase curve of Hilbert transform of a signal produces fluctuated results of instantaneous frequency. The associated variance is reduced by fitting a quadratic polynomial through phase curve in a least-square sense. The instantaneous natural frequency variation of the structure calculated for various load levels is shown Figure 3.15.



**Figure 3.15 Instantaneous frequency variation at different load levels**

It can be observed in Figure 3.15 that the instantaneous natural frequency of the structure is decreasing with time. The gradual decrease in natural frequency is attributed to the gradual stiffness degradation of the structural members. Note here that the instantaneous frequency curves of adjacent load levels are discontinuous at the end points because only the part of a signal is selected for the analysis and the acceleration signal data for

intermediate load levels is not considered in this study. It would be a nearly continuous curve if data for the intermediate levels were used for analysis. For illustration, instantaneous frequency variation of the structure calculated at load levels of three consecutive levels of  $3\text{m/s}^2$ ,  $3.5\text{m/s}^2$ ,  $4\text{m/s}^2$  is shown in Figure 3.16. It can be observed that the instantaneous frequency curve is nearly continuous and the instantaneous frequency of the structure is continuously decreasing.

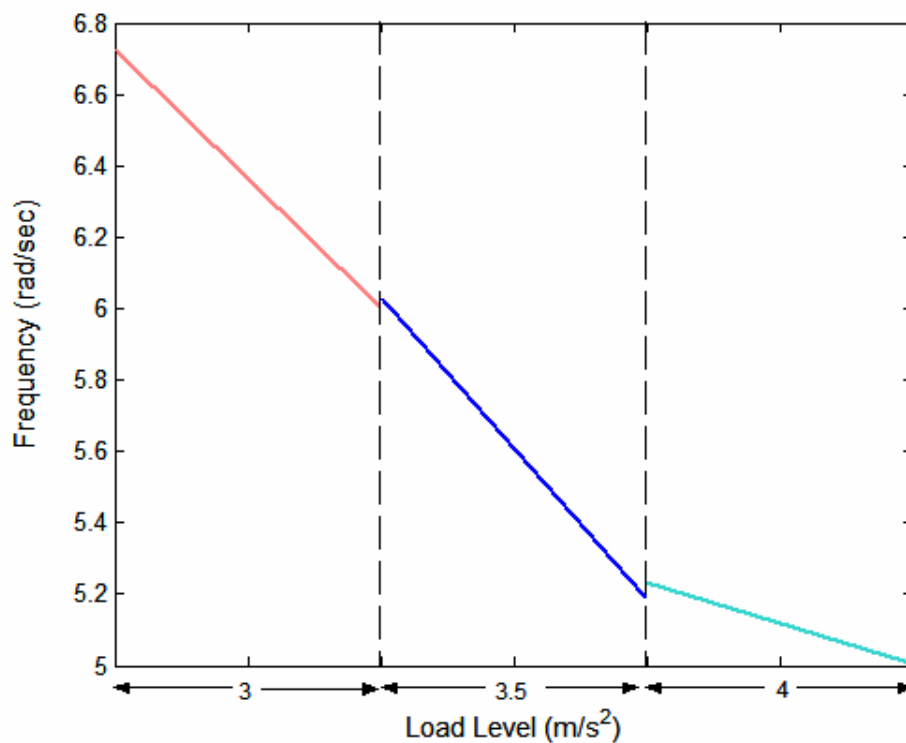


**Figure 3.16 Instantaneous frequency variation at consecutive load levels**

A sudden damage is characterized by sudden stiffness loss which may result in sudden change in instantaneous natural frequency. Because of polynomial curve fitting in order to smooth out the phase curve, a sudden damage in the structure could not be located in the current study. Note here that the decomposed component is a convolution integral of an excitation signal and structural response. In order to locate a sudden damage with non-

stationary forced excitation signal, a structural response must be deconvolved from the acceleration signal collected at different floors of the structure.

The results obtained in numerical as well as experimental studies proves that the wavelet packet sifting process in conjunction with Hilbert transform can be implemented to assess structural health condition. The modal components can be sifted out by using wavelet packet sifting process and, the instantaneous frequency and normalized mode shape information can be obtained from the modal components sifted out with help of Hilbert Transform. The instantaneous frequency and normalized mode shape changed when damage was introduced in the structure.

## 4. COMPARISON STUDY

This section presents a comparative study of the effectiveness of the proposed wavelet packet based damage detection methodology with other two popular damage detection techniques namely Continuous Wavelet Transform (CWT), and Empirical Mode Decomposition (EMD) method. In all of these techniques, a structural health condition is assessed by monitoring a change in natural frequencies and normalized mode shapes. CWT method can be used to identify these instantaneous modal parameters by the wavelet ridges whereas using the EMD method, intrinsic mode functions (IMF) can be sifted from a vibration signal. Instantaneous modal information can be extracted by incorporating the EMD method with the Hilbert Transform. These techniques are illustrated for simulated vibration data from a three-degree-of-freedom system subjected to (i) sudden damage and (ii) progressive damage. The aspects related to the implementation algorithms, sensitivity to damage type and the robustness issues in case of noisy data are discussed.

### 4.1 METHODOLOGY

This section presents a brief background of the methodology behind the techniques of interest in the study.

#### 4.1.1 Continuous Wavelet Transform Method

In CWT technique, the wavelet ridges are used in order to identify the normalized instantaneous mode-shapes and instantaneous natural frequencies. Each ridge on the map of the modulus of CWT corresponds to an instantaneous vibration mode. The mother wavelet chosen in the present study is the complex Morlet wavelet which has a Gaussian

window in both time and frequency domains. Its parameters are the center frequency  $F_c$  and the bandwidth parameter  $F_b$ .

The identification procedure is summarized as follows. The relevant details can be found in (Hera and Hou, 2004). First one needs to identify the  $i^{\text{th}}$  ridge  $a_{\text{ridge}}(t)$  which corresponds to the  $i^{\text{th}}$  time-varying vibration mode. The instantaneous damped natural frequency  $\omega(t)$  can be calculated by Equation 4.1.

$$\omega(t) = \frac{2\pi F_c}{a_{\text{ridge}}(t)} \quad (4.1)$$

Finally, the normalized instantaneous mode shape is calculated by Equation 4.2.

$$\mathbf{X}_{\text{norm}}^{(i)}(t) = \pm \frac{|W_{x_j}(a_{\text{ridge}}(t), t)|}{|W_{x_p}(a_{\text{ridge}}(t), t)|}, j = 1 \cdots N \quad (4.2)$$

$W_{x_j}(a_{\text{ridge}}(t), t)$  represents the wavelet coefficients on the  $i^{\text{th}}$  ridge of the CWT of the signal  $x_j$ . Note that in Equation 4.2, the plus sign is selected if the denominator and the numerator are in phase and vice versa.

#### 4.1.2 Wavelet Packet based Sifting Process

The methodology explained in Section 2.2 is used to separate the modal components and corresponding modal information for structural health monitoring. The instantaneous frequency and normalized mode shapes are calculated by using the equation 3.3 and 3.4 respectively.

#### 4.1.3 Empirical Mode Decomposition Technique

The EMD method decomposes the vibration response into intrinsic mode functions, which are mono-frequency components. The sifting process implemented to sift out these

IMFs is well described in (Huang et al, 1996). Of the interest in present study are the time-varying modal parameters of the system, such as the instantaneous natural frequency and normalized instantaneous mode shape, so in order to extract the modal information, the analytic function is constructed.

The analytic function  $z(t)$  of a signal  $s(t)$  is a complex signal having the original signal  $s(t)$  as its real part and Hilbert transform of the original signal as its imaginary part, expressed as follows:

$$z(t) = s(t) + jH[s(t)] = a(t)e^{i\phi(t)} \quad (4.3)$$

Here  $a(t)$  is the instantaneous amplitude and  $\phi(t)$  is the instantaneous phase function. The instantaneous frequency can be calculated by differentiating  $\phi(t)$  as

$$\omega(t) = \frac{d\phi(t)}{dt} \quad (4.4)$$

The normalized instantaneous mode shape at location ‘j’ with respect to location ‘p’ is obtained by calculating the amplitude ratio  $a_j(t)/a_p(t)$  where  $a_j(t)$  and  $a_p(t)$  are the amplitude of the analytic signal of the mono-frequency component extracted from the free vibration response at location “j” and “p”, respectively.

## 4.2 RESULTS

The instantaneous frequency and normalized mode shape results under different damage scenarios and noise conditions are shown here.

### 4.2.1 Simulation Setup

In the present study, a three-degree-of-freedom system as shown in Fig. 2.1 is employed.

The system is excited by a ‘1\*dt’ impact force of magnitude 1000N applied at mass M3.

The acceleration response at each mass is measured. Two damage cases, as shown in Fig. 4.1, are considered herein:

Case 1: - gradual stiffness degradation. The stiffness of spring K1 was reduced by 40% during a time interval of 10 to 30s.

Case 2: - sudden damage, simulated by an abrupt reduction of 40% in the spring stiffness K1 at  $t = 10$ s.

The natural frequencies of the healthy system are 1.29, 3.62, 5.23 Hz which reduced to 1.10, 3.35, 5.14 Hz respectively after a 40% stiffness loss of spring K1. The fairly large change in stiffness value is employed here in order to have a clear perspective of the methods compared.

The measurement noise is simulated as a Gaussian white noise process with a zero mean and standard deviation equal to a certain percentage of the root mean square (RMS) value of the acceleration response at M3 over the whole time interval.

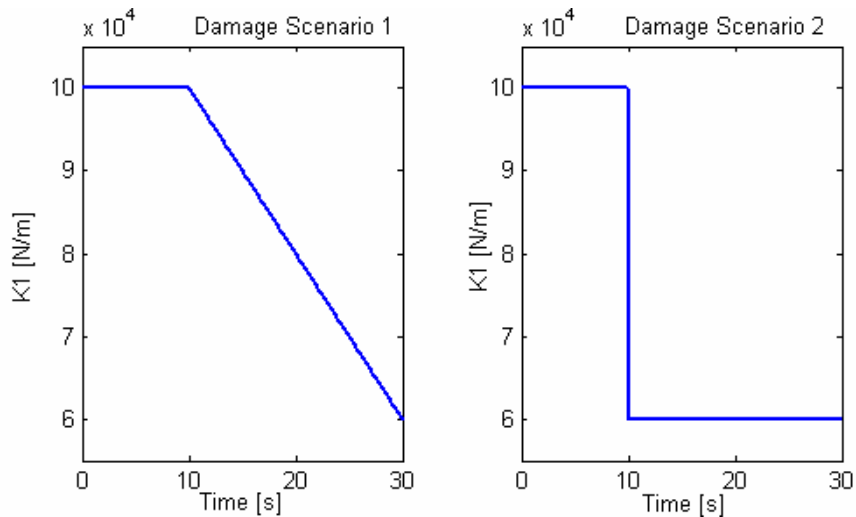


**Figure 4.1 Stiffness history for: a) damage scenario 1, b) damage scenario 2**

### **4.2.2 Implementation of the Methods**

For CWT, the complex Morlet wavelet with normalized center frequency  $F_c=5$ , and normalized bandwidth parameter  $F_b=1$  was chosen as mother wavelet. The scale range employed was from 10 to 500.

In case of WPS, db36 was used as the analyzing mother wavelet in data decomposition. Each sifted mono-frequency component was transformed into an analytic signal in order to identify the instantaneous frequency and amplitude.

In order to obtain the physically meaningful modal components by EMD method, a sifting algorithm defined in (Huang et al, 1996) is used in conjunction with a band pass filter technique illustrated in (Yang et al, 2004). The necessity of incorporating a band pass filter with the sifting process is discussed in Appendix- A.

In case of gradual damage, the oscillations introduced, while computing the instantaneous frequency and amplitude results obtained with all these methods, are smoothed out by a filtering technique. However, in order to keep the essence of the abrupt change, in case of a sudden damage this smoothing technique is not applied to the modal parameter data.

### **4.2.3 Simulation Results**

By implementing each method the instantaneous frequencies and normalized instantaneous mode shape vectors are calculated. The normalization is done with respect to the component corresponding to mass M1, therefore the normalized mode shape component for M1 have a constant unity value over the whole time interval. For a comparison purpose all of the results obtained with different methods are plotted on same graph.

For validation of the results, the modal parameters obtained by solving the associated eigen-value problem at each time step are plotted as reference and denoted by “MA” on the plots. Since the change of system parameters is relatively slow with respect to the natural frequencies of the system in case of progressive damage, while in case of a sudden damage the system is piecewise time invariant, the reference parameters calculated by solving an eigen-value problem at each time step are justified.

#### ***4.2.3.1 Progressive Damage***

Fig. 4.2 plots the instantaneous normalized mode shape components corresponding to mass M2 and M3, while Fig. 4.3 illustrates the instantaneous natural frequency corresponding to the first vibration mode. The same set of data corresponding to the second vibration mode is presented in Fig. 4.4 and 4.5.

All results are in good agreement with the reference normalized mode shape and frequency values, except in the end regions due to the end effects observed in relevant methods.

In this study, the third vibration mode is not utilized for identifying damage, as due to its high damping ratio this mode decays very fast and practically the associated modal information can not be employed for damage identification.

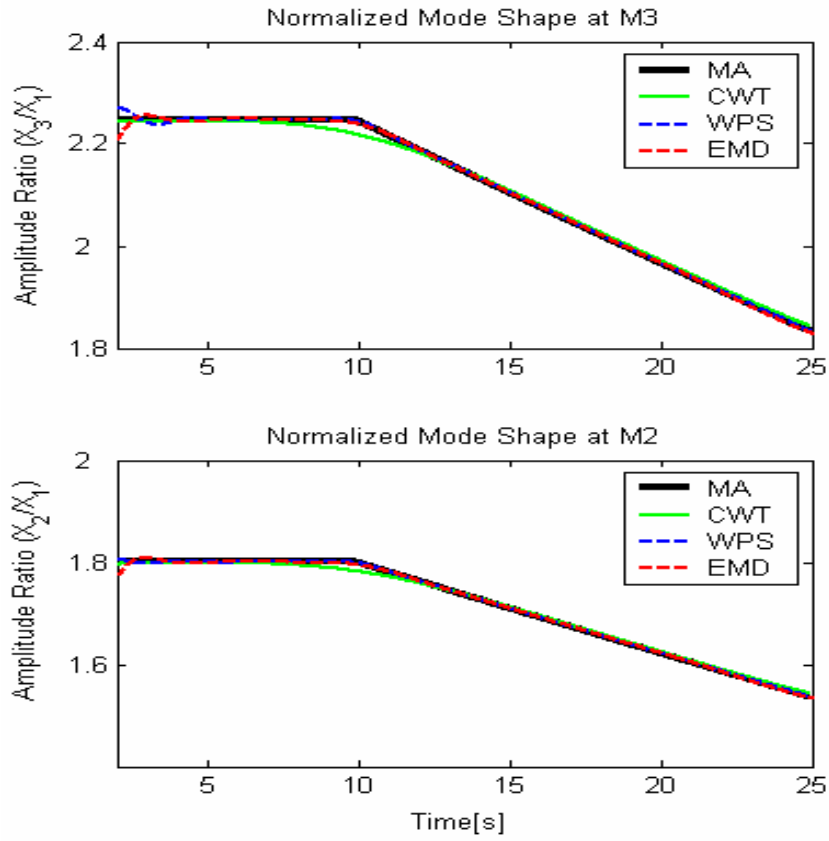


**Figure 4.2** The normalized instantaneous mode shape for the first vibration mode, damage scenario 1, no measurement noise.

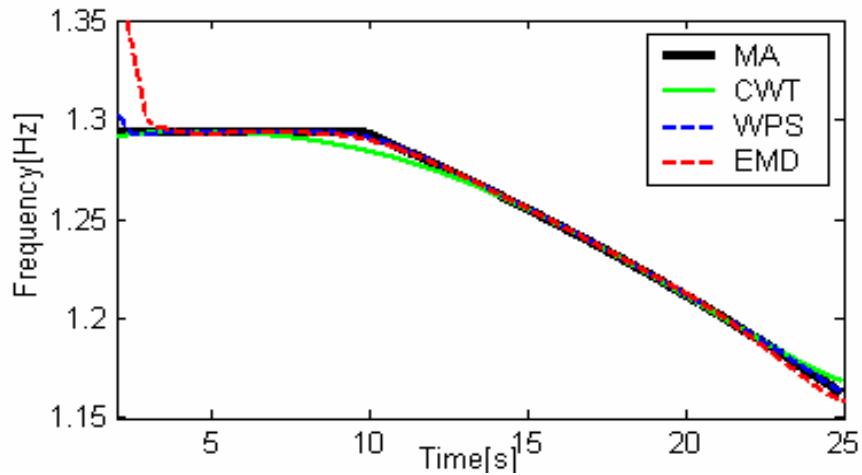


**Figure 4.3** The instantaneous damped natural frequency for the first vibration mode, damage scenario 1, no measurement noise.

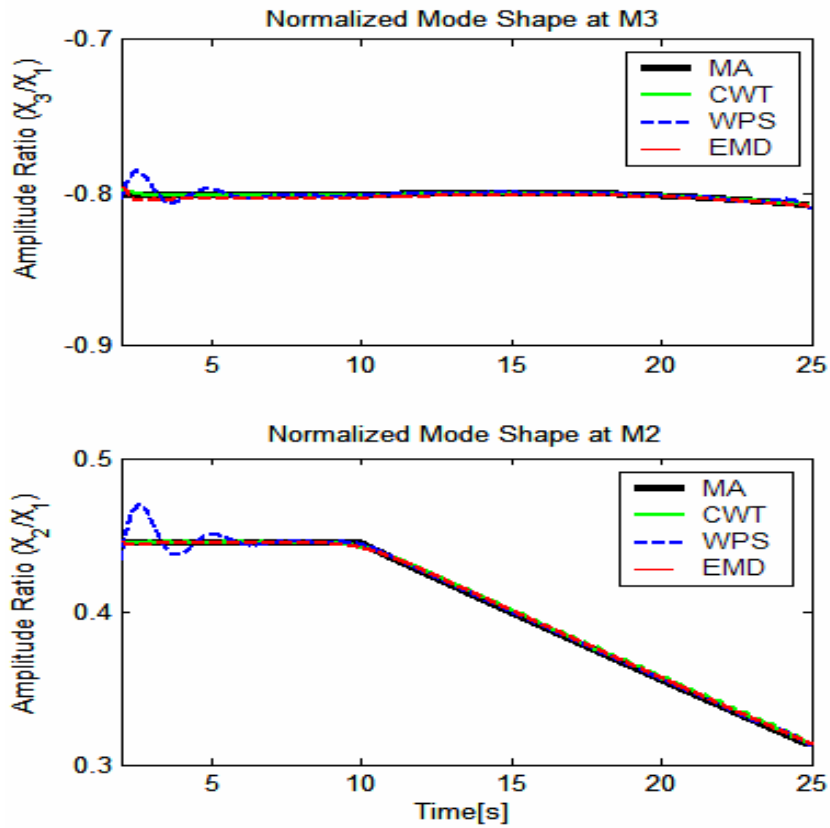


**Figure 4.4** The normalized instantaneous mode shape for the second vibration mode, damage scenario 1, no measurement noise.

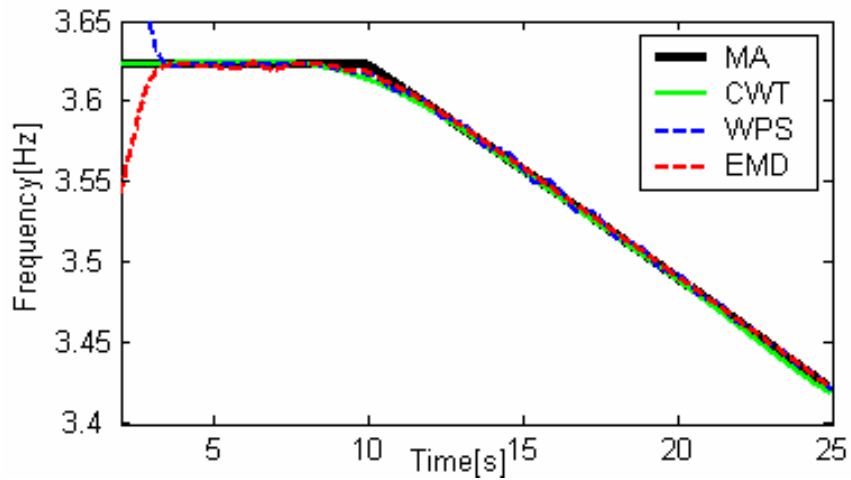


**Figure 4.5** The instantaneous damped natural frequency for the second vibration mode, damage scenario 1, no measurement noise.

### 4.2.3.2 Sudden Damage

The results for the instantaneous modal parameters corresponding to the first vibration mode in case of sudden damage are shown in Fig. 4.6 and 4.7.

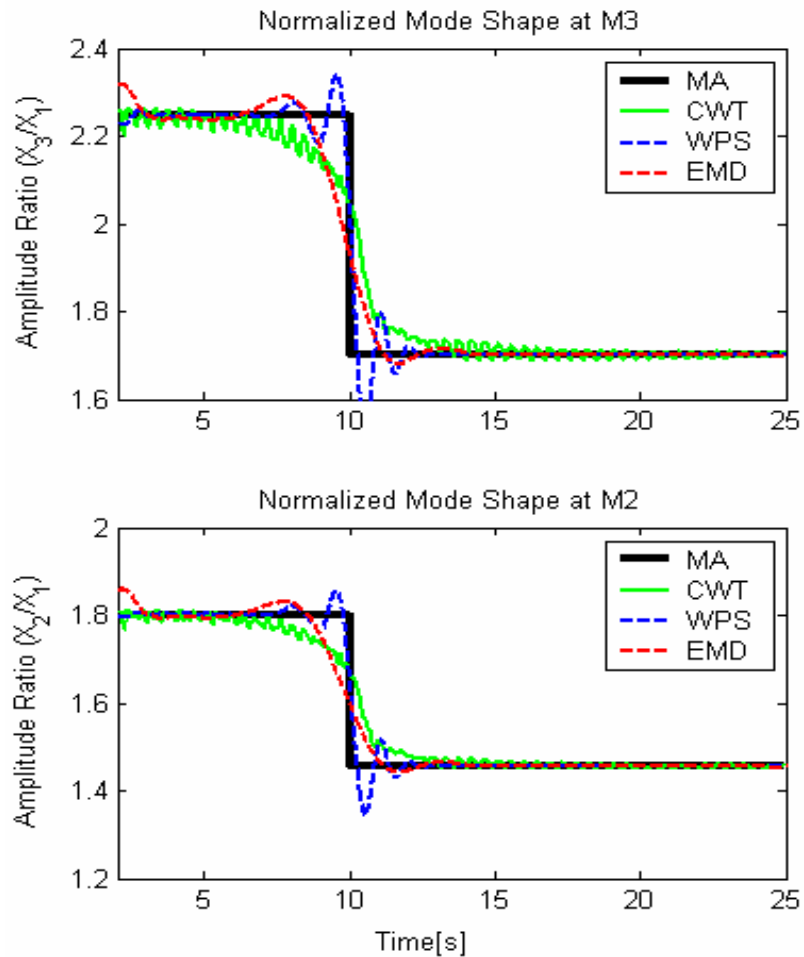


**Figure 4.6** The normalized instantaneous mode shape for the first vibration mode, damage scenario 2, no measurement noise.

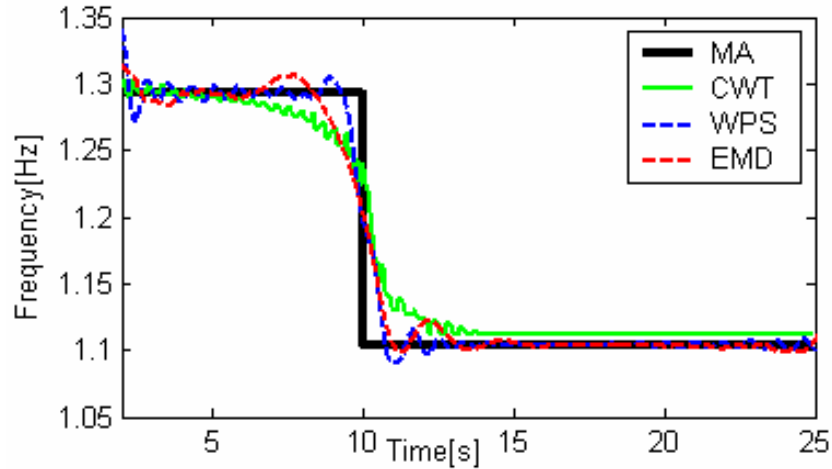


**Figure 4.7 The instantaneous damped natural frequency for the first vibration mode, damage scenario 1, no measurement noise.**

The WPS technique could effectively identify the abrupt change in the system parameters and the results are well localized on time axis. The HHT method could monitor the change in modal parameters but observed to be less effective in time localization. In case of CWT method, at the scales corresponding to the first vibration mode the size of the wavelet is larger and therefore CWT method gradually adapts to the changes.

#### **4.2.4 Damage Detection in Presence of Measurement Noise**

The effectiveness of each method in presence of measurement noise is illustrated in Fig. 4.8 and 4.9 for monitoring gradual damage and in Fig. 4.10 and 4.11 for a case of sudden damage. The simulated acceleration signals were contaminated by a 5% measurement noise. As can be seen, there is not much difference in the instantaneous frequency results but normalized mode shape results show small deviations from the reference values.

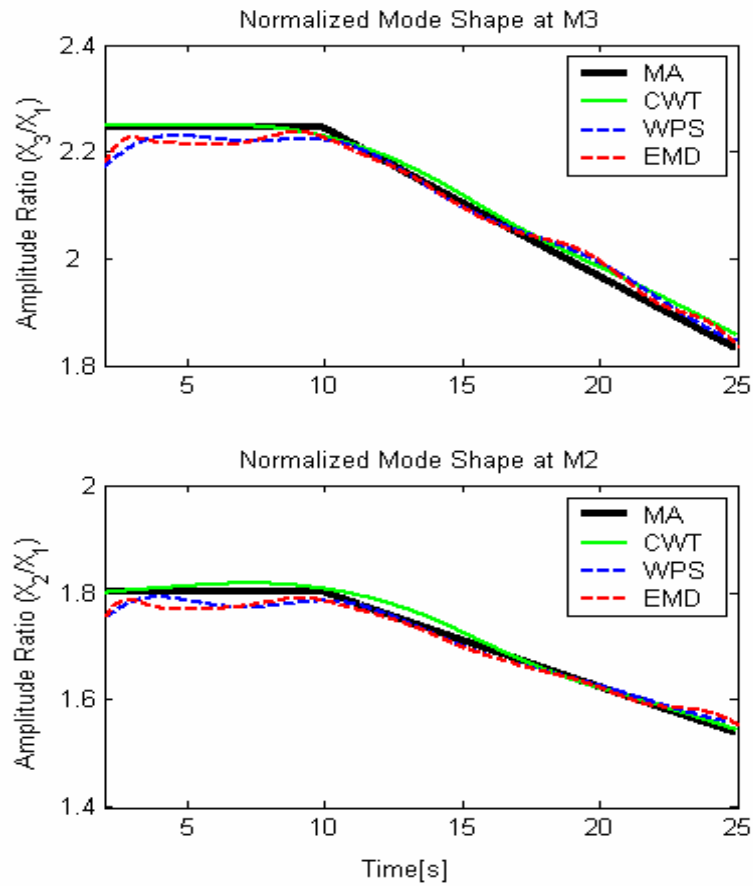


**Figure 4.8** The normalized instantaneous mode shape for the first vibration mode, damage scenario 1, measurement noise level=5%.

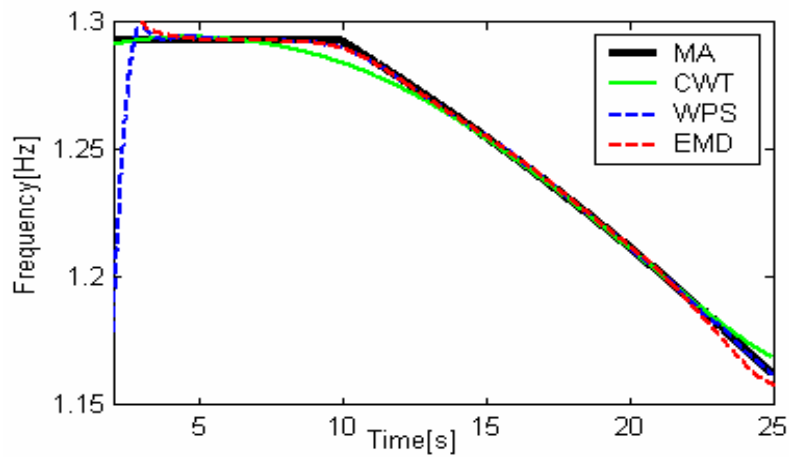


**Figure 4.9** The instantaneous damped natural frequency for the first vibration mode, damage scenario 1, measurement noise level=5%.

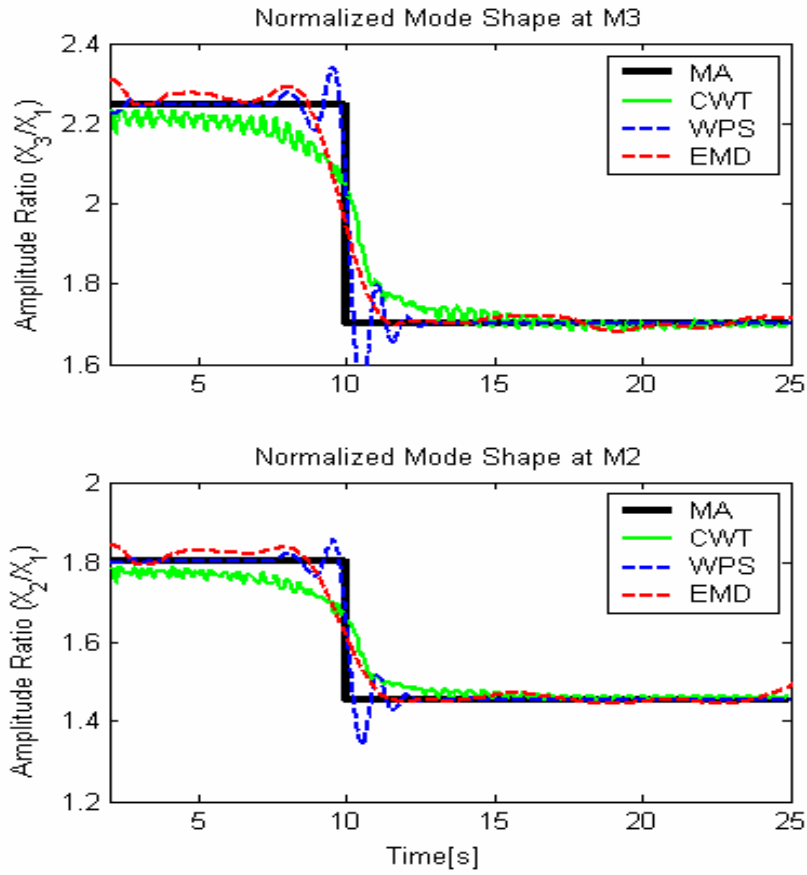


**Figure 4.10** The normalized instantaneous mode shape for the first vibration mode, damage scenario 2, measurement noise level=5%.

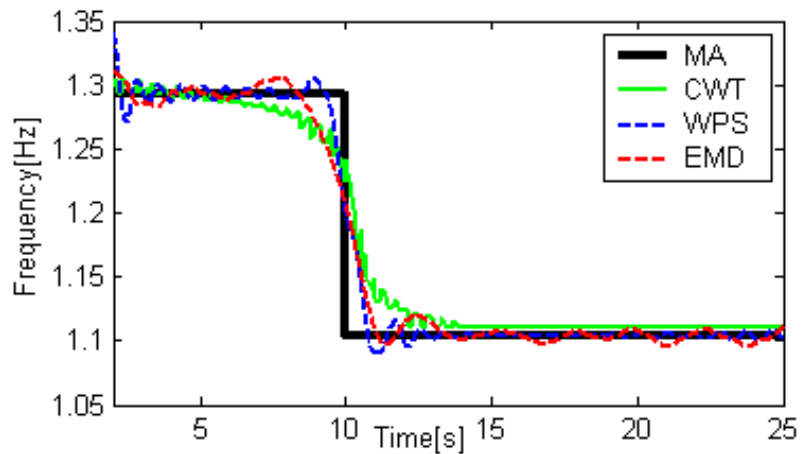


**Figure 4.11** The instantaneous damped natural frequency for the first vibration mode, damage scenario 2, measurement noise level=5%.

## **4.3 DISCUSSION**

### **4.3.1 Interpretation of the Methods**

In case of CWT, a one-dimensional signal in time domain is represented in a two dimensional space of time and scale. For a given mother wavelet, the transformation is done under a well established mathematical formulation. Then, the useful modal information is extracted from the modulus and phase maps in the time-scale domain. For a selected mother wavelet, e.g. the Morlet wavelet in this paper, there is mathematical relationship between the wavelet ridges on the map and the instantaneous natural frequency and normalized mode shape.

In case of the WPS method, the time varying mono-frequency components of the signal are reconstructed based on a wavelet packet sifting process. Once, the analyzing mother wavelet is selected this decomposition is unique. The time varying modal components of the signal are characterized by high energy content. By combining it with the Hilbert transform, this technique can be used to track the instantaneous modal parameters.

The EMD method consists of a sifting process to decompose a signal into a set of the IMFs. The sifting process is based on subjective criteria such as envelope definition and stopping criteria. Because of the absence of the mathematical formulation of this method, one cannot guarantee that the IMFs obtained are the same as the modal components of the signal. In order to obtain the mono-frequency components corresponding to each vibration mode in the sifting procedure a band-pass filtering needs to be implemented in the original sifting process. However, for time varying systems, the

selection of the bandwidth should be made carefully in order to prevent a leakage of modal components and possibility of false interpretation of damage.

### **4.3.2 Robustness to Noise**

CWT map comprises a lot of redundant data which emphasize the information of interest in the signal. With an efficient method for ridge detection the method seems to be very robust to noise. WPS method shows very good results for abrupt damage in this study, however in case of high intensity noise, the results for modal parameters need a filtering which may reduce the time localization capability of this method. In case of EMD method, the band pass filtering is a part of the sifting process which makes the method tolerant to high noise levels.

Figures 4.8 and 4.10 show the deviation of computed normalized instantaneous mode shapes from the reference values. This may be attributed to the loss of information regarding the modal parameters results while filtering. As a general conclusion, due to its redundant nature, the CWT method could give better results in case of noisy measurements.

The instantaneous natural frequency results remained unaffected with noise as seen in Figure 4.9 and 4.11 in case of each method. It is evident that the measurement noise affects the normalized mode shape results whereas shows comparatively small effect on the natural frequency results.

### **4.3.3 Sensitivity to the Damage Type**

WSP approach gives good results in both damage cases, and time localization in case of sudden damage is better than the results obtained with CWT and EMD method. The WPS

method identifies the abrupt changes quite effectively, as long as the CWT requires a long time to accommodate the changes due to its limited time resolution. For lower frequencies, in other words at high scales, the wavelet window is large, which in turn limits the time localization. Changing the mother wavelet parameters, e.g. the center frequency and the bandwidth parameter, should be done carefully as long as a good frequency localization implies a poor time localization and vice a versa. In case of sudden damage, EMD partly loses its capability to monitor abrupt change in system parameters as seen in the Fig. 4.6 and 4.7. This is due to the band pass filtering introduced in the sifting process in order to improve the effectiveness of the method for identifying the modal components of the signal.

In case of gradual damage, as a rate of change of stiffness is very slow, all methods could successfully monitor the change in modal parameters.

In conclusion, all three methods, CWT, WPS, and EMD/HHT with band-pass filter, were successfully applied for detecting both sudden and progressive damage and comparable results were obtained in the present study. It is found that the wavelet ridge function in CWT, the dominant mono-frequency components in WPS, and the IMF in EMD have similar properties in the frequency domain and their inherent connection is under investigation. Based on this similarity, EMD/HHT technique might be viewed as an implicit wavelet analysis and if this view holds the three methods, in fact, provides alternative ways to implement wavelet filters.

However, some differences between these three techniques were observed in this simulation study. For sudden damage case, WPS works better than EMD method, whereas CWT results in poor time localization of damage. For a gradual damage, all

methods performed effectively in monitoring modal parameters. In a situation involving a high level measurement noise, CWT may be a better choice among these methods. Factually, CWT and WPS are backed up by the well-established mathematical theory of wavelet analysis and wavelet packet analysis, which facilitates their implementation and physical interpretation of the results obtained. In contrast, a direct EMD provides an efficient and robust procedure to decompose a signal into its IMFs, whose physical significance is sometimes difficult to interpret, as reported in the literature. This may be partially attributed to the empirical nature of the procedure and subjective definition of IMFs and envelopes involved. Other techniques such as filters need to be incorporated with it to improve the performance for SHM applications.

For a practical application, selection among these methods should be based on the damage type and the noise level involved. A robust framework for damage detection may be developed either by making a parallel use of these methods or by implementing a methodology incorporating all these methods in an efficient way.

## 5. CONCLUSION

The proposed wavelet packet based sifting process can successfully decompose a signal into components with simple frequency content. By choosing a regularized analyzing wavelet and appropriate decomposition criteria, the sifting process decomposes the vibration response into physically meaningful monocomponents. The sifting process shows comparable results as EMD method and performs better in certain cases analyzed.

This sifting process can be used for assessing health of a time-varying structure by monitoring instantaneous modal parameters of the corresponding structure. When applied for a free vibration response of a structure, the proposed sifting process results into modal components. The instantaneous modal information i.e. natural frequency and instantaneous mode shape can be extracted from the decomposed modal components with help of Hilbert Transform. The methodology can be effectively used for detecting sudden damage as well as gradual stiffness degradation. The instantaneous natural frequency and normalized mode shape change its value when damage occurs and the change is in proportion to the damage severity.

The experimental results showed that the method can be effectively used for assessing structural health where the instantaneous natural frequency of the wooden structure decreased gradually with increasing load levels. The information about sudden damage was lost because of curve fitting but idea about damage in structure could be obtained.

The comparison study showed that for sudden damage case, the proposed method works better than CWT and EMD technique, whereas for a progressive damage case, all methods showed similar results. The method also effectively detected both types of

damages in presence of measurement noise and showed robustness in case of noisy measurement data. The EMD method has to be modified to effectively use for SHM.

In conclusion, the proposed wavelet packet based sifting process showed its effectiveness for signal decomposition and its application for SHM by successfully detecting both, sudden as well as gradual stiffness degradation, even in presence of measurement noise, in numerical as well as experimental studies.

## 6. FUTURE WORK

In this work it is shown that in case of structure subjected to impulse as well as harmonic excitation, if the modes are well separated, the natural frequency as well as normalized mode shapes can be accurately calculated. But in case of earthquake excitation, when the structure is subjected to a non-stationary base excitation and the structure is a time-varying system, the free vibration response of the structure is difficult to be extracted from the transient response signal and exact monitoring of natural frequency and normalized mode shape becomes difficult. Due to the time-varying system, the classical Fourier based deconvolution can not be applied to deconvolve the free vibration response from the structural response. A non-stationary deconvolution method can be developed which may help to accurately monitor the instantaneous modal parameters.

The methodology is applied for a numerical as well as experimental data. More experiments can be conducted to evaluate the effect of damage intensity and measurement noise level. The effectiveness of the method can be further evaluated by applying it for a real seismic response data of structures measured during an earthquake event.

As the method is developed for a non-stationary signal analysis, the effectiveness of the proposed method can be further improved by combining it with other adaptive signal analysis techniques e.g. Adaptive Kalman Filter technique and Adaptive Neural Network technique.

## REFERENCES

- Adeli, H., (2001), "Neural networks in civil engineering: 1989-2000", *Computer-Aided Civil and Infrastructure Engineering*, 16(2), pp. 126-142.
- Allen, J. B., and Rabiner, L. R., (1977), "A Unified Approach to Short-time Fourier Analysis and Synthesis," *Proc. IEEE*, 65(11), pp. 1558-1564
- Boashash B., (1992), "Estimating and Interpreting the Instantaneous Frequency of a Signal Part 1: Fundamentals", *Proceedings of the IEEE*, 80(4), pp. 520-537.
- Brincker, R., Kirkegaard, P., Anderson, P., and Martinez, M., (1995a), "Damage Detection in an Offshore Structure," *Proc. of the 13th International Modal Analysis Conference*, 1, pp. 661-667.
- Chang, C.C., Sun, Z., 2001, "Continuous Condition Assessment for Bridges Based on Wavelet Packet Decomposition", *Proceedings of SPIE - The International Society for Optical Engineering*, 4337, pp. 357-367
- Chen, H., Tsai, K., Qi, G., Yang, J., and Amini, F., (1995), "Neural Network for Structure Control", *Journal of Computing in Civil Engineering*, 9(2), pp. 168-176.
- Chiang L., Russell E. and Braatz R., (2001), "Fault Detection and Diagnosis in Industrial Systems", Springer Verlag.
- Coifman, R., and Wickerhauser, M., (1992). "Entropy based Algorithms for Best Basis Selection", *IEEE Trans. Information Theory*, 38, pp. 713-718.
- Daubechies, I., (1992), "10 Lectures on Wavelets", Capital City Press.
- Dellomo, M., (1999), 'Helicopter gearbox fault detection: a neural network based approach', *Journal of Vibration and Acoustics, Transactions of the ASME*, 121(3), pp 265-272.
- Doebling, S., Farrar, C., Prime, M., and Shevitz, D., "Damage Identification and Health Monitoring of Structural and Mechanical Systems from Changes in Their Vibration Characteristics: A Literature Review," 1996, *Los Alamos National Laboratory Report LA-13070-MS*.
- Flandrin, P., Rilling, G., and Goncalves, P., (2004), "Empirical Mode Decomposition as a Filter Bank," *IEEE Sig. Proc. Lett.*, 11(2), pp. 112-114.

- Ghanem, R., Romeo, F., (2000), "A wavelet-based Approach for the Identification of Linear Time-Varying Dynamical Systems", *Journal of Sound and Vibration*, **234**(4), pp.555-576.
- Goswami, J., and Chan, A., (1999), "Fundamentals of Wavelets: Theory, Algorithms and Applications", Wiley-Interscience.
- Haykin, S., (1998). "Neural Networks: A Comprehensive Foundation (2<sup>nd</sup> Edition)", Pearson Education.
- Hera A., and Hou Z., (2003). "Application of Wavelet Approach for ASCE Structural Health Monitoring Benchmark Studies", *ASCE Journal of Engineering Mechanics* **130**(1), pp. 96-104.
- Hera, A. and Hou, Z., (2003), "Detecting Progressive Damage by Wavelet Approach", *Journal of Sound and Vibration*, (submitted)
- Hou, Z., Noori S. and Amand, St. R., (2000). "A Wavelet-Based Approach for Structural Damage Detection", *ASCE Journal of Engineering Mechanics*, **126**, pp. 667-683.
- Hou, Z., (2001), "Wavelet-Based Damage Detection Techniques and Its Validation using Shaking Table Test Data of a Wooden Building Structure", *Disaster Prevention Research Institute, IMDR Research Booklet No. 3A*.
- Hou, Z., Hera, A., Liu, W., Hendrickson, D., (2003), "Identification of Instantaneous Modal Parameters of Time-varying Systems Using Wavelet Approach", *The 4th International Workshop on Structural Health Monitoring*, Stanford University, CA
- Mini-Symposium on Hilbert-Huang Transforms in Engineering Applications*, (2003), October 31- November 1, Newark, Delaware, <http://www.ce.udel.edu/HHT/>.
- Huang et al, (1998), "The Empirical Mode Decomposition Method and the Hilbert Spectrum for Non-linear and Non-stationary Time Series Analysis", *Proc. R. Soc. Lond*, **454**, pp. 903-995.
- Kerezsi, B., and Howard, I., (1995), "Vibration Fault Detection of Large Turbo-generators using Neural Networks", *IEEE International Conference on Neural Networks - Conference Proceedings*, **1**, pp. 121-126.
- Kijewski, T., Kareem, A., (2003), "Wavelet Transforms for System Identification in Civil Engineering", *Computer-Aided Civil and Infrastructure Engineering*, **18**(5), pp. 339-355.

- Kijewski, T., Kareem, A., (2002), "On the Presence of End Effects and their Melioration in Wavelet-based Analysis", *Journal of Sound and Vibration*, **256**(5), pp.980-988.
- Lam, H.F., Katafygiotis, L.S., and Mickleborough N.C., (2004), "Application of a Statistical Model Updating Approach on Phase I of the IASC-ASCE Structural Health Monitoring Benchmark Study", *Journal of Engineering Mechanics*, 130(1), pp. 34-48.
- Lei et al, (2003), "An Enhanced Statistical Damage Detection Algorithm Using Time Series Analysis", *Proceedings of the 4th International Workshop on Structural Health Monitoring*, Stanford, CA, USA.
- Liang, Y., Zhou, C., and Wang Z., (1997), "Identification of restoring forces in non-linear vibration systems based on neural networks", *Journal of Sound and Vibration*, 206(1), pp 103-108.
- Lus, H., Betti, R., Longman, R.W. (1999). "Identification of Linear Structural Systems using Earthquake-Induced Vibration Data", *Journal of Earthquake Eng and Structural Dynamics*, **28**, pp.1449 –1467.
- Mallat, S., (1998), "A Wavelet Tour of Signal Processing". Academic Press.
- Nelles, O., (2000), "Nonlinear System Identification: From Classical Approaches to Neural Networks and Fuzzy Models", Springer-Verlag.
- Osegueda, R., Dsouza P., and Qiang, Y., (1992), "Damage Evaluation of Offshore Structures Using Resonant Frequency Shifts", *Serviceability of Petroleum, Process, and Power Equipment*, ASME PVP **239** /MPC **33**, pp. 31–37.
- Pandey, A., and Biswas, M., (1994), "Damage Detection in Structures Using Changes in Flexibility", *Journal of Sound and Vibration*, **169** (1), pp. 3–17.
- Paya, B., Esat, I., Badi, M., (1997), "Artificial Neural Network based Fault Diagnostics of Rotating Machinery using Wavelet Transforms as a Preprocessor", *Journal of Engineering and Applied Science*, 11(5), pp. 751-765.
- Piombo, B.A.D., Fasana, A., Marchesiello, S., Ruzzene, M., (2000), "Modeling and Identification of the Dynamic Response of a Supported Bridge", *Mechanical Systems and Signal Processing*, **14**(1), pp. 75-89.
- Prasad L. and Iyengar S., (1997). "Wavelet Analysis with Applications to Image Processing", CRC Press: Boca Raton.

- Rioul, O., and Vetterli, M., (1991), "Wavelets and Signal Processing", *IEEE SP Magazine* 8(4), pp. 14-38.
- Ruzzene, M., Fasana, A., Garibaldi, L., Piombo, B., 1997, "Natural Frequency and Damping Identification Using Wavelet Transform: Application to Real Data", *Mechanical Systems and Signal Processing*, **11**(2), pp. 207-218.
- Rytter, A., (1993), "Vibration Based Inspection of Civil Engineering Structures", *Ph. D. Dissertation, Department of Building Technology and Structural Engineering, Aalborg University, Denmark.*
- Saadat S., (2003), "Structural Health Monitoring and Detection of Progressive and Existing Damage using Artificial Neural Networks-Based System Identification", *PhD Dissertation*, <http://www.lib.ncsu.edu/theses/available/etd-03052003-025350/>.
- Salawu, O. and Williams, C., (1993), "Structural Damage Detection Using Experimental Modal Analysis—A Comparison of Some Methods", *Proc. of 11th International Modal Analysis Conference*, pp. 254–260.
- Samanta, B., Al-Balushi, K., and Al-Araimi, S., (2004), "Bearing Fault Detection Using Artificial Neural Networks and Genetic Algorithm", *Eurasip Journal on Applied Signal Processing*, 2004(3), pp 366-377.
- Shimizu et al, (2001), "Full Scale Vibration Tests of Two Storied Wood Houses by Post and Beam Structure, Experimental Results of Post-and-Beam Frames with Braces", *Summaries of Technical Papers of 2001 Annual Meeting, Architectural Institute of Japan.* (in Japanese).
- Silva, J. and Gomes A., (1994), "Crack Identification of Simple Structural Elements Through the use of Natural Frequency Variations: The Inverse Problem", *Proc. of the 12th International Modal Analysis Conference*, pp. 1728–1735.
- Smith, S., and Beattie, C., (1991a), "Model Correlation and Damage Location for Large Space Truss Structures: Secant Method Development and Evaluation", NASACR-188102.
- Sohn, H., and Farrar, C., (2001), " Damage Diagnosis Using Time Series Analysis of Vibration Signals", *Smart Materials & Structures*, 10 (3), pp. 446-451.

- Sohn, H., Farrar, C., Hunter, N., Worden, K., (2001a), "Structural Health Monitoring using Statistical Pattern Recognition Techniques", *Jour. Dyn. Sys. Meas. & Control, Trans. ASME*, 23 (4), pp. 706-711.
- Sohn, H., Farrar, C., Hunter, H. and Worden, K., (2001b), "Applying the LANL Statistical Pattern Recognition Paradigm for Structural Health Monitoring to Data from a Surface-Effect Fast Patrol Boat". *Los Alamos National Laboratory Report, LA-13761-MS*.
- Staszewski, W. J., (1998), "Structural and Mechanical Damage Detection Using Wavelets", *The shock and Vibration Digest*, 30, pp. 457-472.
- Sun, Z., Chang, C. C., (2002), "Structural Damage Assessment Based on Wavelet Packet Transform", *Journal of Structural Engineering*, **128**(10), pp. 1354-1361.
- Ville, J., (1948), "Theorie et application de la notion de signal analytical", *Cables et Transmissions 2A-1*, pp. 61-74.
- Vincent, B., Hu, J., and Hou, Z. (1999), "Damage Detection Using Empirical Mode Decomposition Method and a Comparison with Wavelet Analysis", *Proceedings of the Second International Workshop on Structural Health Monitoring, Stanford*, pp. 891-900.
- Yang, J., and Lei, Y., (2000), "System Identification of Linear Structures Using Hilbert Transformation and Empirical Mode Decomposition", *Proceedings of 18<sup>th</sup> International Modal Analysis Conference, A Conference on Structural Dynamics, San Antonio I*, pp. 213-219.
- Yang, J.N. and Lei, Y., (2000), "System Identification of Linear Structures Using Hilbert Transformation and Empirical Mode Decomposition", *Proceedings of 18<sup>th</sup> International Modal Analysis Conference, A Conference on Structural Dynamics, San Antonio, TX, I*, pp. 213-219.
- Yang, J.N., Lei, Y., Pan, S., Huang, N., (2003), "System Identification of Linear Structures based on Hilbert-Huang Spectral Analysis. Part I: normal modes", *Earthquake Engineering & Structural Dynamics*, **32**(9), pp. 1443-1467.
- Yang, J.N., Lei, Y., Pan, S., Huang, N., (2003), "System Identification of Linear Structures based on Hilbert-Huang Spectral Analysis. Part II: Complex Modes", *Earthquake Engineering & Structural Dynamics*, **32**(10), pp. 1533-1554.

- Yang, J.N, Lei, Y., Lin,S., Huang, N. , (2004), “Hilbert-Huang-Based Approach for Structural Damage Detection” , *Journal of Engineering Mechanics*, **130**(1), pp. 85-95.
- Yang, J.N. and Lei, Y., (2000), “System Identification of Linear Structures Using Hilbert Transformation and Empirical Mode Decomposition”, *Proceedings of 18<sup>th</sup> International Modal Analysis Conference*, A Conference on Structural Dynamics, San Antonio, TX, I, 213-219.
- Yen, G.G., and Lin, K.C., (2000), “Wavelet Packet Feature Extraction for Vibration Monitoring”, *IEEE Trans. Industrial Electronics*, 47(3), pp. 650-667.
- Yuen, K., Au, S., and Beck, J., (2004), “Two-Stage Structural Health Monitoring Approach for Phase I Benchmark Studies”, *Journal of Engineering Mechanics*, 130(1), pp. 16-33.
- Yuen, K., Beck, J., Katafygiotis, L.S., (2002), “Probabilistic Approach for Modal Identification using Non-stationary Noisy Response Measurements Only”, *Earthquake Engineering and Structural Dynamics*, 31, pp. 1007-1023.
- Yuen, K., Beck, J., Katafygiotis, L.S., (2002), “Bayesian Model Updating using Complete Input and Incomplete Response Noisy Measurements”, *Journal of Engineering Mechanics*, 128(3), pp. 340-350.
- West, W., (1984), “Illustration of the Use of Modal Assurance Criterion to Detect Structural Changes in an Orbiter Test Specimen”, *Proc. Air Force Conference on Aircraft Structural Integrity*, pp. 1–6.
- Worden, K., Allen, D., Sohn, H., Stinematers, D. and Farrar C., (2002). “Extreme Value Statistics for Damage detection in Mechanical Structures”, *Los Alamos National Laboratory Report, LA-13903-MS*.
- Zimmerman, D., and Smith, S., (1992), “Model Refinement and Damage Location for Intelligent Structures”, *Intelligent Structural Systems*, H.S. Tzou and G.L. Anderson, Eds., Kluwer Academic Publishers, pp. 403–452.

## APPENDIX A - THE MODIFIED EMD METHOD

With the EMD method, because of a lack of mathematical formulation, one can not guarantee that the sifting process will decompose the vibration response into its modal components. Figure A-1 illustrates the fact where the EMD method applied to the vibration response at location M1 (Figure 2.1) resulted in IMFs characterized by a combination of different modes whereas ideally it should result in three distinct modal components. The IMF1 obtained is a combination of second and third mode components whereas IMF2 is a combination of first and second mode. A part of first mode can be seen in IMF3.

In order to obtain the physically meaningful modal components by EMD method, a sifting algorithm defined in is used in conjunction with a band pass filter technique described in Yang et al (2003). The results obtained by employing band-pass filters with the EMD method are shown in Fig. A-2, where the method successfully decomposed the same signal into three distinct modal components. IMF1, IMF2 and IMF3 corresponds to the third, second and first vibration mode respectively.

It illustrates the fact that the band-pass filter must be incorporated with the EMD method for SHM applications based on monitoring the system modal parameters.

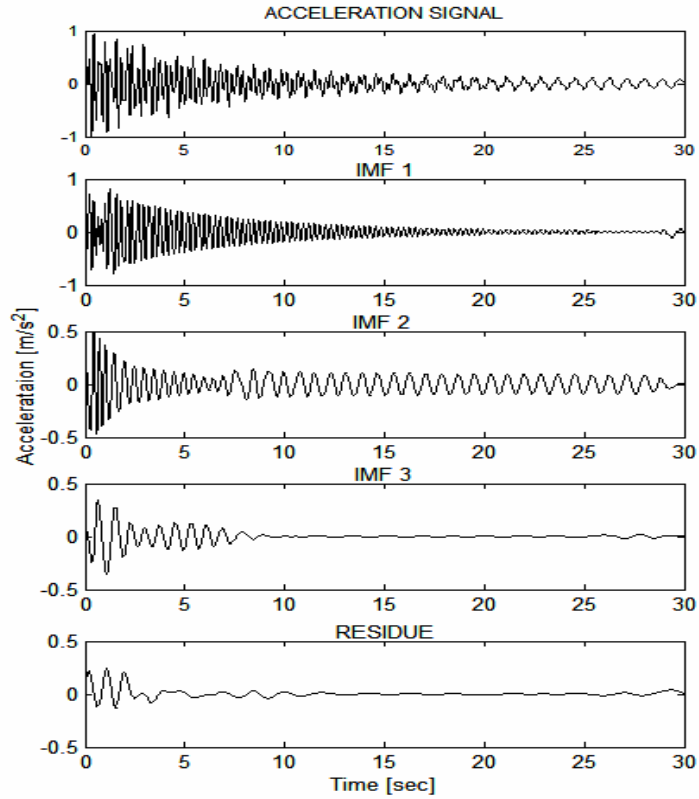


Figure A1 Decomposition results obtained by EMD method

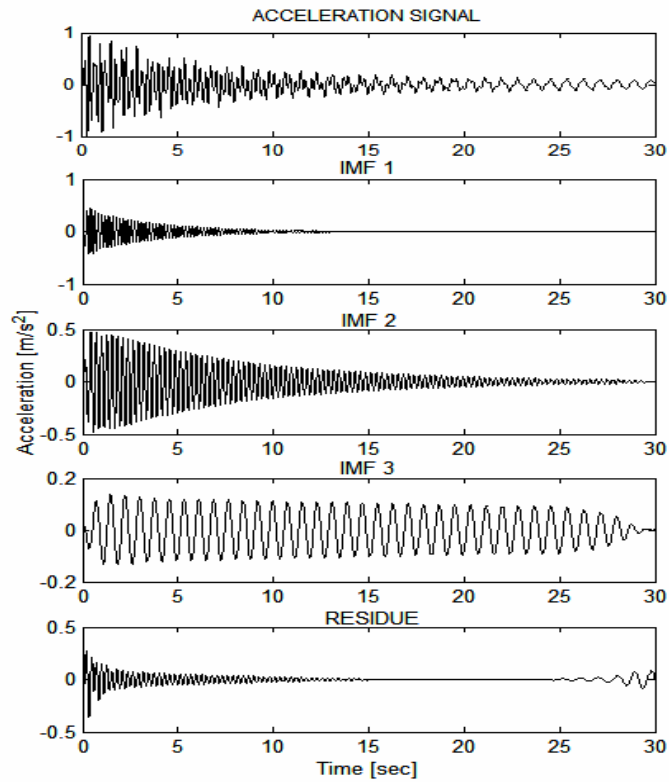


Figure A2 Decomposition results obtained by modified EMD method